Department of Mechanical Engineering
SDSU - College of Engineering

Parabolic Solar Water Distillation

Senior Design Project
Interim report

Team Members:

Andrew Stonebraker
Joel Newmeyer
Mark Branner

Advisors: Dr. Fletcher Miller
Dr. Kee Moon

Special Thanks: Akasha Kaur Akasha

Table of Contents

Purpose

The purpose of this project is to design a water distillation system that can purify water from nearly any source, a system that is relatively cheap, portable, and depends only on renewable solar energy. From the results of project calculations a truthful estimate was made to prototype the most effective geometries of the distiller and trough concentration system, one that will maximize evaporation/condensation and re capture waste heat to minimize thermal losses.

Abstract

The motivation for this project is the limited availability of clean water resources and the abundance of impure water available for potential conversion into potable water. Our project goal is to efficiently produce clean drinkable water from solar energy conversion. To achieve this goal, a system was designed incorporating a parabolic solar trough coupled with a custom designed distillation device. The incoming solar radiation from the sun is focused and concentrated onto a receiver pipe using a parabolic trough, heating the incoming impure water, at which point it is sprayed into our custom designed distillation device where it evaporates and is re-condensed into pure potable water. Future goals for this project include calculation refinement, material research/testing, and fabrication.

Introduction and Background

Motivation and Importance

About 70% of the planet is covered in water, yet of all of that, only around 2% is fresh water, and of that 2%, about 1.6% is locked up in polar ice caps and glaciers. So of all of the earth's water, 98% is saltwater, 1.6% is polar ice caps and glaciers, and 0.4% is drinkable water from underground wells or rivers and streams. And despite the amazing amount of technological progress and advancement that the current world we live in has undergone, roughly 1 billion people, or 14.7% of the earth's population, still do not have access to clean, safe drinkable water. A few of the negative results of this water crisis are:

- Inadequate access to water for sanitation and waste disposal
- Groundwater over drafting (excessive use) leading to diminished agricultural yields
- Overuse and pollution of the available water resources harming biodiversity
- Regional conflicts over scarce water resources

In addition to these problems, according to WaterPartners International, waterborne diseases and the absence of sanitary domestic water is one of the leading causes of death worldwide. For children less than 5 years old, waterborne disease is THE leading cause of death, and at any given moment, roughly half of all hospital beds are filled with patients suffering from water-related diseases. Clearly, having affordable potable water readily available to everyone is an important and pressing issue facing the world today.

Needs and Specifications

Our project centers on converting the roughly 99.6% of water that is, in it's natural form, undrinkable, into clean and usable water. After researching and investigation, we outlined our needs to be the following:

- Efficiently produce at 2 gallons of potable water per day minimum
- Able to purify water from virtually any source, included the ocean
- Relatively inexpensive to remain accessible to a wide range of audiences
- Easy to use interface
- Intuitive setup and operation
- Provide clean useful drinking water without the need for an external energy source
- Reasonably compact and portable

Our aim is to accomplish this goal by utilizing and converting the incoming radioactive power of the sun's rays to heat and distill dirty and undrinkable water, converting it into clean drinkable water. A solar parabolic trough is utilized to effectively concentrate and increase the solid angle of incoming beam radiation, increasing the efficiency of the system and enabling higher water temperatures to be achieved.

Literature Review

For a complete summary of the various literatures used and considered during the planning and research portions of our project can be found in Appendix A.

Articles/Research Papers/Documents

Fresh Water from Sea Water by Solar Distillation, May 1953. Maria Telkes.

- Useful data on amount of solar energy received on a surface as well as methods of calculating solar energy required for solar distillation

Solar trough concentration for fresh water production and waste water treatment, 9 Feb. 2007. Scrivani, El Asmar, and Bardi.

- Information related to application of solar troughs in use of water treatment
- Very similar to our project design specification

Sun and water: an overview of solar water treatment devices. May 1998. Trudy Rolla.

- Benchmark: Florida Solar Energy Center utilizes a solar trough with concentric copper pipes for heat exchange
    - 92 sq. ft concentrator
    - Capable of producing up to 660 gal/day
    - Cost: $1,680 w/o the cost of pumps and reservoirs

Performance of a parabolic trough solar collector. August 2006. Journal of Energy in Southern Africa.

- Helpful study containing equations and charts for calculating thermal efficiency, collector acceptance angle, incident angle modifier, and thermal losses

Manual making of a parabolic solar collector. 2007. Gang Xiao.

- Useful and practical design methods for making a single solar collector
- Relevant materials used in making of small scale collectors

Parabolic Trough Collector Overview. 2007. Dr. David W. Kearney.

- Information pertaining to current large scale parabolic trough installations
- Benchmark for geometry, material, orientation of troughs
- Approximate cost of trough material costs

Review of Mid- to High-Temperature Solar Selective Absorber Materials. July 2002. C.E. Kennedy.

- Technical report containing research on the performance of various types of parabolic trough receiver surface coatings and their applications
- Information on the effect on efficiency of various surface texturing methods

Loss	Open trough	Closed trough	Comments
Cover reflection loss	1	0.95	Open trough has no cover. Closed trough has a cover with anti-reflection treatment.
Mirror reflectivity	0.93	0.93	Equal quality mirrors.
Glass tube reflection loss	0.95	0.95	Equal quality tubes, treated anti-reflection.
Intercept factor	0.98	0.98	Equal optical precision supposed.
Receiver absorptivity	0.95	0.95	Equal quality receiver surface.
Incidence angle cos effect	0.82	0.99	Open trough is horizontally installed, latitude 40°. Closed trough is optimally tilted north-south axis, with tilting angle adjusted 2 or 4 times a year.
End and join loss	0.9	1	Open trough has end loss and loss on receiver supporting structure. No such losses for closed trough.
Glass tube multiple travel	0.995	0.99	A small amount of light travels several times through the glass tube. This is slightly more important for the closed trough due to a glass tube of larger diameter.
Dust loss	0.94	0.98	Light to an open trough travels 3 times through dust-coverable surfaces. Only once for closed trough.
Row-to-row shading	0.98	0.95	Closed trough deliberately adopts a more condensed row-to-row distance, prompted by its lower cost, in order to reduce land use and piping cost. The data result from a computer simulation taking into account the atmospheric attenuation and the Sun's angle.
Thermal capacity	0.95	0.99	The big open trough has a thicker receiver, hence a higher thermal capacity per unit aperture area. Heat corresponding to the thermal capacity is lost after sunset or cloud coverage. The thermal capacity is 0.36Wh/m^2·K, or 126Wh/m^2 for a temperature elevation of 350°C. Assuming an average collection of 2.5kWh/m^2 per period of sunshine, the loss represents 5%. This loss is 6 times less for the smaller closed trough.
Efficiency before thermal loss	52.8%	70.6%	Efficiencies above are multiplied; loss below is subtracted.
Thermal loss	10%	10%	Assume 800W average incoming light intensity and 80W/m^2 thermal loss for both cases.
Final efficiency	42.8%	60.6%	This is the efficiency with respect to direct normal insolation.

Table 1. *: Parabolic trough efficiency comparison*

System Type	Characteristic & Use	Advantages	Disadvantages
Solar Batch Water Heater *(ICS)*	Open loop; Integrated collector & storage; Freeze protection generally limited to infrequent or light freeze climates $6000–	Simple; No moving parts; *Passive*	600 pounds on roof Inefficient in cold climates; *Higher roof load* cold water supply
Thermosyphon	May be closed loop with heat exchanger & antifreeze $6500–	Simple; Requires no electricity for operation; *Passive*	Collector must be located below tank; *Higher roof load* Water pipes exposed to freezing.
Direct Pump Recirculation System	Open loop; Climates where freezing is an unexpected occasion open loop direct forced	Simple; can be powered by PV; *Active* *(needs AC power for proper freeze protection)*	Freeze protection is limited to infrequent & light freezes; Inappropriate for use with hard water NO!
Closed Loop Heat Exchanger	Antifreeze on roof in cold Closed loop; Cold climates ask for steam flush $7000	Very good freeze protection; Basic principles well understood by conventional plumbing trades; No problems with hard water; can be powered by PV; *Active*	Heat exchanger & antifreeze reduce efficiency; Fluid may break down at high stagnation temperatures maintenance 40% glycol to 60% water @ 5yrs
Drainback	Closed loop; Cold climates; *Designed to drain water when near freezing or overheating* most expensive	Very good freeze protection if used with antifreeze; No problems with hard water; Simplest of reliable freeze protection systems; Fluid not subject to stagnation temperatures; can be powered by PV; *Active*	more parts Heat exchanger & antifreeze reduce efficiency; Collectors & piping must have adequate slope to drain; Requires larger pump to lift

Source: Arizona Solar Center, http://www.azsolarcenter.com/technology/solarh20.html/ Items in *italics* added by CCSE

Table 2. Solar Water Heating System Types: Pros and Cons.

lated tank HX Propylene Glycol closed loop collector

CAD Models

The distillation geometry was chosen to maximize the amount of condensate (potable water) that can be extracted from the system. The cylinder design was to maximize surface area for evaporation yet provides some flexibility when accounting for heat losses. The cone heat exchanger above the condensing surface is to provide a surface heat exchanger that will preheat the incoming cool dirty water by cooling the hot condensing surface, which helps keep the condensation rate inside the distiller effective.

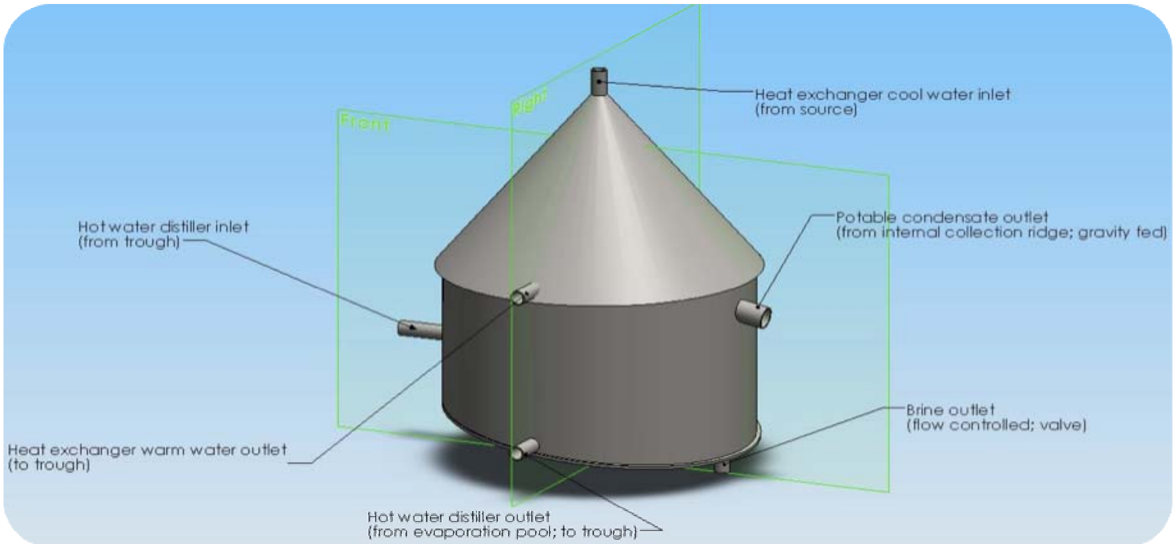

Figure 1. Distiller.

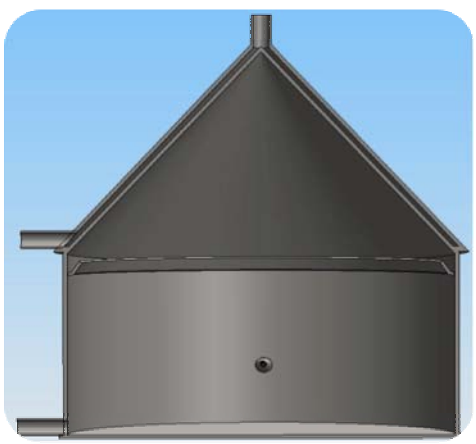

Figure 2. Distiller front sectional view.

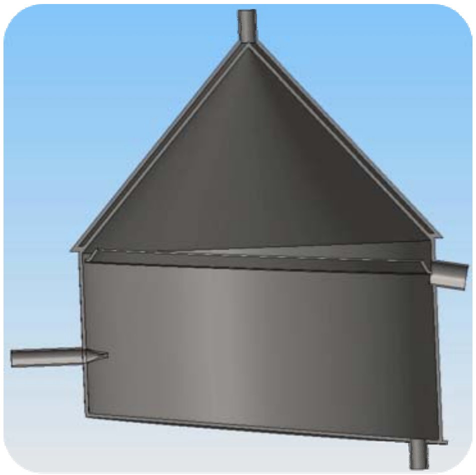

Figure 3. Distiller right sectional view.

As shown in Figure 3 a sloped lip coincides with the inner wall of the distiller at a slight angle to allow for condensate to effectively drain into a collection pipe.

In order to try and maximize the evaporation inside the distiller a spray nozzle was proposed to increase the surface area per droplet of water/water vapor entering the distiller from the trough receiver heat pipe.

The bottom surface of the distiller is sloped to allow for brine (waste) water to drain out at a controlled rate with a control valve.

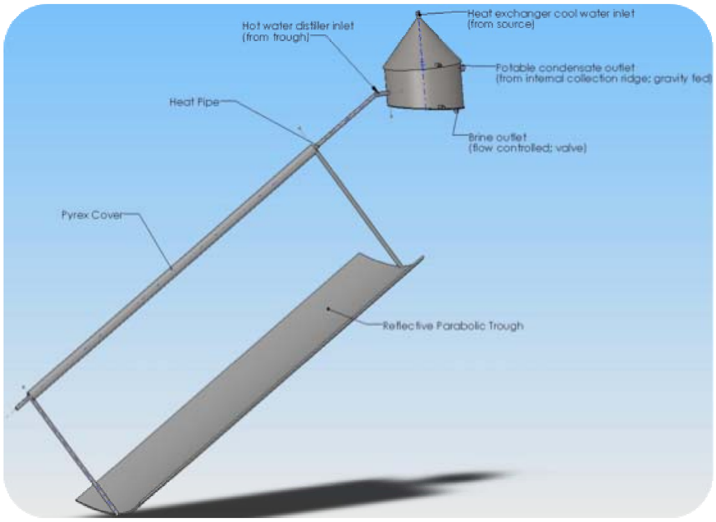

Figure 4. Trough and distiller simple assembly. To be added; support structure, pump, PV panel, piping, and storage tanks.

One obstacle that the project has is the film thickness and distribution of the incoming heat exchange fluid over the cone shaped condensing surface. Surface tension makes water difficult to work with in this geometry. As a possible solution the use of grooves carved into the heat exchange side of the condensing surface to allow channels for the water to flow thus allowing for constant even distribution of cooling or the use of a fabric to distribute the water over the surface were proposed.

Calculations and Interpretations

The data presented is based on simulations, modeling, approximations, and theoretical calculation of a chosen trough/distillation system for San Diego, Ca (latitude 32 deg N). This data will then be used to design a final parabolic trough distillation system.

For simplification we assumed the trough to have a horizontal axis, because it allows for a more conservative approximation, however we plan to angle the trough collector at an angle equal to the regions latitude, which will increase the average energy gain per meter.

Available Energy

There are many ways to measure the available radiation from the sun. Most commonly used is a pyranometer, which measures diffuse plus beam radiation from the sky and sun. These devices measure absorbed radiation by detecting the temperature difference between two concentric silvered rings, one coated in magnesium oxide and the other Parson’s black [1].

Solar insolation is defined as average intensity (radiation per solid angle) or the measure of solar radiation received on a surface at some time. Average insolation on the Earth's surface is approximated to be 250 W/m^2 or 6 kWh/m^2/day.

- 1 kWh/m²/day = 1,000 W * 1 hour / (1 m² * 24 hours) = 41.67 W/m²

Measurements of available solar energy were made with a pyranometer located at San Diego State University's field station. Measurements were recorded every 15 minutes for 15 days; see Figure 1.

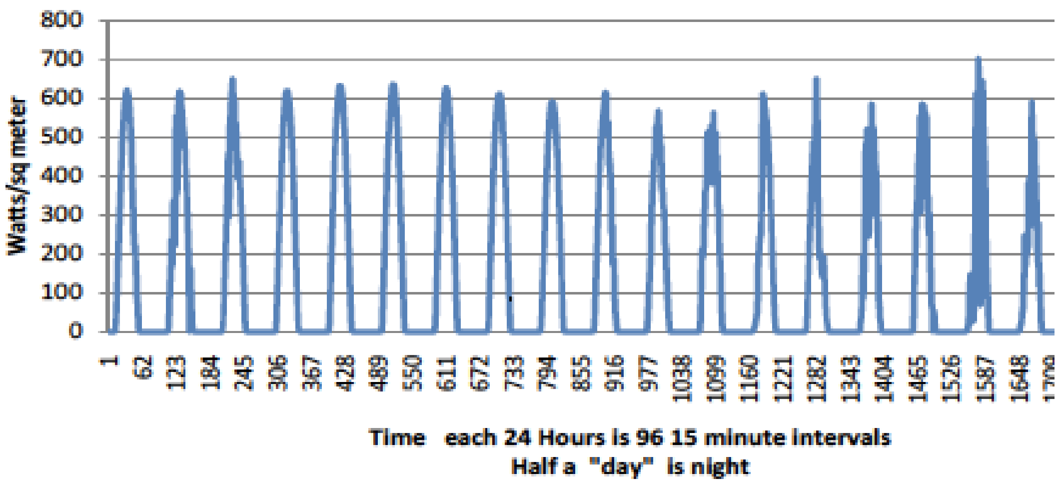

Figure 5. Solar radiation data taken from SDSU field station [2].

Since pyranometer's measure diffuse and beam radiation, more information was required because concentrating collectors can utilize only beam radiation. For this reason additional data was acquired for San Diego (latitude 32 deg N) from an online Redbook posted by the National Renewable Energy Laboratory. The data presented is organized exclusively into beam radiation for concentrating collectors for various axis/tracking configurations, as shown in Figure 2.

```
DIRECT BEAM SOLAR RADIATION FOR CONCENTRATING COLLECTORS (kWh/m2/day), Percentage Uncertainty = 8"
"Tracker   ","          ","Jan","Feb","Mar","Apr","May","Jun","Jul","Aug","Sep","Oct","Nov","Dec","Year"
"1-X, E-W ","Average", 3.8, 3.8, 3.9, 4.3, 3.9, 4.0, 4.9, 4.8, 4.2, 4.1, 4.0, 3.8, 4.1
"Hor Axis ","Minimum", 2.4, 2.5, 2.9, 3.4, 2.5, 1.8, 2.9, 3.8, 1.9, 3.0, 2.7, 2.5, 3.6
"          ","Maximum", 4.9, 5.1, 5.3, 5.5, 5.2, 5.7, 5.8, 5.6, 5.2, 5.2, 5.2, 4.8, 4.5
"1-X, N-S ","Average", 3.1, 3.8, 4.6, 5.6, 4.9, 5.0, 6.2, 6.1, 5.1, 4.4, 3.6, 3.0, 4.6
"Hor Axis ","Minimum", 2.0, 2.3, 3.4, 4.3, 3.1, 2.3, 3.6, 4.7, 2.3, 3.2, 2.4, 2.0, 3.9
"          ","Maximum", 4.1, 5.1, 6.3, 7.1, 6.8, 7.3, 7.4, 7.2, 6.3, 5.5, 4.6, 3.8, 5.0
"1-X, N-S ","Average", 4.2, 4.7, 5.1, 5.7, 4.7, 4.7, 5.8, 6.1, 5.5, 5.2, 4.6, 4.1, 5.0
"Tilt=Lat ","Minimum", 2.7, 2.9, 3.8, 4.4, 3.0, 2.1, 3.4, 4.7, 2.5, 3.8, 3.1, 2.7, 4.3
"          ","Maximum", 5.4, 6.2, 7.0, 7.3, 6.5, 6.8, 7.0, 7.2, 6.8, 6.5, 6.0, 5.2, 5.4
"2-X       ","Average", 4.5, 4.8, 5.1, 5.8, 5.0, 5.1, 6.2, 6.3, 5.5, 5.3, 4.9, 4.5, 5.3
"          ","Minimum", 2.9, 3.0, 3.8, 4.5, 3.2, 2.3, 3.7, 4.9, 2.5, 3.8, 3.3, 3.0, 4.5
"          ","Maximum", 5.8, 6.4, 7.1, 7.4, 6.9, 7.3, 7.5, 7.4, 6.9, 6.6, 6.3, 5.7, 5.7
"AVERAGE CLIMATIC CONDITIONS"
```

Figure 6. Data acquired from National Renewable Energy Laboratory redbook [3].

With the data presented an average daily insolation of 522 W/m^2 was used for the system design calculations.

Trough Geometry

The amount of solar radiation collected is highly dependant on the geometry of the trough, which acts as our aperture for solar collection. This can be observed with the concentration ratio, C [1];

$$C = \frac{A_a}{A_r} \qquad 1$$

The aperture area is directly proportional to the concentration ratio. This means that the higher the concentration ratio the higher the temperatures that can be reached. This is because the number of images, formed by the reflection of sunlight, seen by the receiver pipe will increase. However, the objective of this system is to heat water to vaporization, and not to produce high quality steam; therefore a medium concentration ratio is used. The chosen system produces a concentration ratio of about 12.

For the trough analysis first a basic shape was introduced as follows,

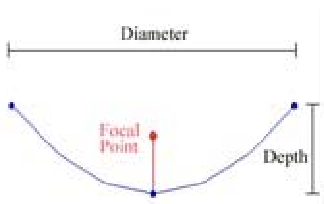

Diameter = 25 in
Focal length = 19.5 in
Depth = 2 in
f/a = 19.5 in / 25 in = 0.78

Now, analysis of the solar image size and ultimately ideal receiver diameters are done. This analysis is to maximize the amount of radiation the receiver pipe can absorb.

Some key terms include the rim radius and rim angle which directly correlate to aperture size, thus a larger rim radius and smaller rim angle will maximize solar collection. However, the larger the rim radius the larger the focal length will be, and the larger the image will be (means a larger receiver pipe will be needed and thus thermal losses increase).

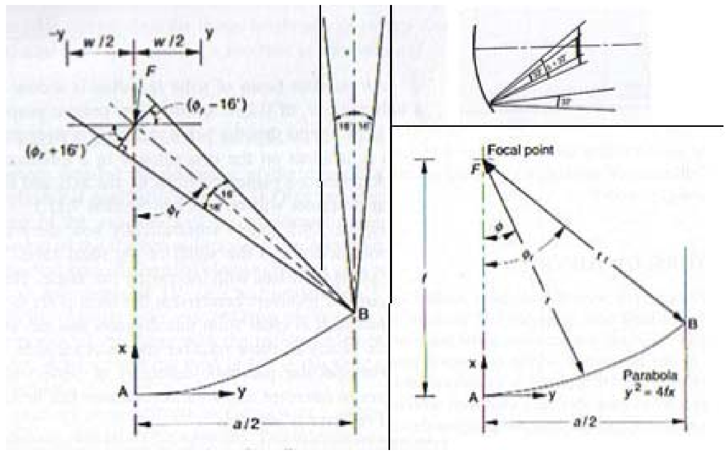

Figure 7. The left Illustrates the effects of the solar solid angle, because the sun is not a point source the image produced at the focal point has width (focal plane), and is a function of trough geometry, The top right shows the dispersion angle to account for trough imperfections, The bottom right shows the parabolic shape, focal length, rim radius, and rim angle [1].

The rim radius and rim angle are found as follows;

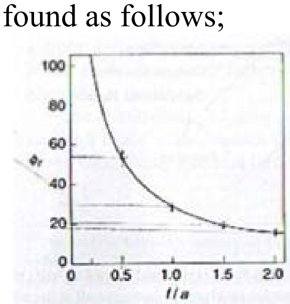

Figure 8. Graph showing the rim angle as a function of focal length-aperture ratio [1].

$$r_r = \frac{2f}{1+\cos\phi_r} \qquad 2$$

Where, f is the focal length and φ_r is the rim angle and is found with the graph in Figure 8. With this information the ideal receiver pipe diameter can be found, one that will capture the entire solar image.

$$D = 2r_r \sin(0.267 + \delta/2) \qquad 3$$

Where, r_r is the rim radius, and δ is the dispersion angle which is used to correct for trough imperfections and should be acquired by the trough manufacturer or looked up in a table. Ultimately the best trough geometry was chosen, as follows

Diameter = 25 in of aperture
19.5 in focal length
21.5 in rim radius
2 in depth
Rim angle = 35.5 degrees
Trough length = 1.3 m = 4.27 ft
$A_{aperature}$ = 0.7826 m^2

$A_{receiver} = 0.064834618\ m^2$
$OD_{receiver} = 0.015875$ m
$ID_{receiver} = 0.013843$ m
$OD_{cover} = 0.033$ m
$ID_{cover} = 0.031$ m

Thermal Performance of Receiver/Cover System

Due to the nature of thermal processes the temperature gradients created by the receiver pipe will generate radiative heat loss to the ambient and sky. In addition, heat is lost by conduction through the support structure. Also, there are convective losses to the ambient from wind as well as the convective losses between the cover and receiver pipes. As a general rule of thumb as the temperature of the receiver increases the heat lost will directly increase as well, this analysis is done as follows.

Energy Balance

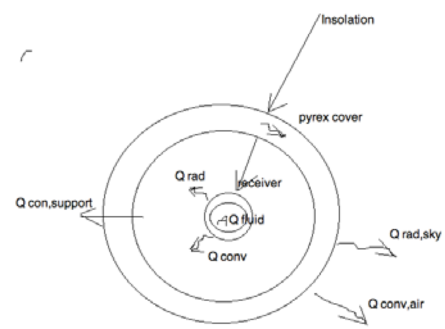

Figure 9. Energy balances on the receiver and cover system.

When analyzing heat lost in a system one first relates incoming energy to outgoing energy into an energy balance [5]. The incoming radiation is from the sun and is as follows,

$$Q_{in} = Q_{solar,1} + Q_{solar,2} \qquad 4$$

Where, $Q_{solar,1}$ is the incoming solar insolation and $Q_{solar,2}$ is the solar radiation that is transmitted through the Pyrex cover, which absorbs some incoming radiation. Equation 4 shows the heat lost or outgoing heat.

$$Q_{loss,tot} = Q_{rad} + Q_{conv} + Q_{rad,sky} + Q_{conv,wind} + Q_{cond,\sup} \qquad 5$$

In the analysis of the overall system the heat lost to the supports through conduction is assumed to be 0. Furthermore the space between the receiver and cover was assumed to be evacuated therefore convective heat losses from the receiver to the cover would be neglected as well. Furthermore, all surfaces are assumed to be smooth.

Convective Wind Losses

This section evaluates heat lost by the cover system to the ambient. This convective loss will depend on the flow pattern across the cover system, turbulent or laminar. Reynolds number directly relates the flow pattern to the wind speed (Equation 7); therefore the convective loss to the wind is variable and always fluctuating. For the purposes of analysis a wind speed of 3.58 m/s (8 mph) was chosen. This number was chosen because ASHRAE testing standards call for analysis to be done with wind speeds between 5-10 mph. Heat loss will also depend on temperature of the cover system thus an evaluation temperature (Equation 6) is used to evaluate the thermal properties of air.

$$T_{evaluation} = \frac{(T_r + T_a)}{2} \qquad 6$$

Where, T_r is the receiver temperature and T_a is the ambient temperature (19 C) both in degrees C. Now the flow pattern across the cover is analyzed as follows.

$$\mathrm{Re} = \frac{\rho V D_{co}}{\mu} \qquad 7$$

Where, Re is the Reynolds number (if Re>1000 then flow = turbulent), ρ is the density of air at $T_{evaluation}$, V is the wind speed in m/s, D_{co} is the outer diameter of the cover, and μ is the kinematic viscosity of air at $T_{evaluation}$. Re for the chosen system yielded a number 1000<Re<50000, thus the Nusselt number and ultimately the heat transfer coefficient can be acquired from turbulent correlations in Equation 7 [4].

$$Nu = 0.3 * \mathrm{Re}^{0.6} = \frac{h_w L}{k} \qquad 8$$

Where, L is the length of the trough and k is the thermal conductivity of air at $T_{evaluation}$.

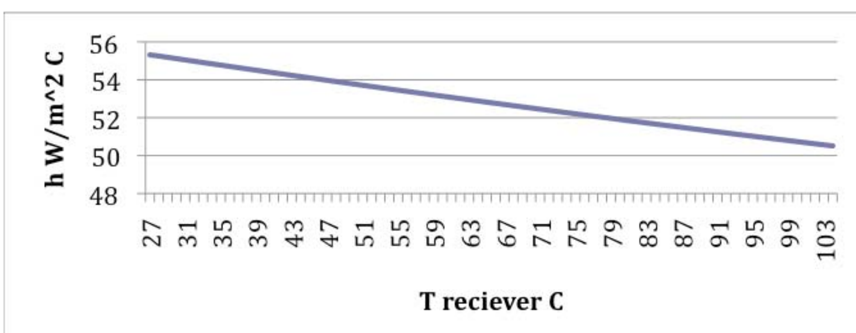

Figure 10. Convective heat transfer coefficient of the wind as a function of receiver temperature.

Overall Heat Loss

The overall heat loss analysis calls for an iterative process, due to the fact that the heat loss is dependent on the temperature of the cover (T_{co}), which is initially unknown and a lot closer to T_a than T_r. Therefore, two heat loss values will be calculated (in Watts), Equation 11 accounts for heat lost from receiver to cover and Equation 9 accounts for heat lost from cover to ambient. These values will be compared and if Equation 9 does not equal Equation 11 ($Q_{loss} \neq Q_{loss}$) then the initial guess of the cover temperature is wrong and another will need to be made until Equation 9 = Equation 11 [1].

$$Q_{loss} = \pi D_{co} L h_w * (T_{co} - T_a) + \varepsilon_c \pi D_{co} L \sigma * (T_{co}^4 - T_{sky}^4) \quad 9$$

$$T_{ci} = T_{co} + \frac{Q_{loss} * \ln \frac{D_{co}}{D_{ci}}}{2\pi k_c L} \quad 10$$

$$Q_{loss} = \frac{\pi D_r L \sigma (T_r^4 - T_{ci}^4)}{\frac{1}{\varepsilon_r} + (\frac{1 - \varepsilon_c}{\varepsilon_c} * \frac{D_r}{D_{ci}})} \quad 11$$

Where, h_w is the wind heat transfer coefficient in W/m^2 C, T_{co} is the temperature of the outside cover surface (initially guessed), ε_r is the emissivity of the receiver surface (0.45), ε_c is the emissivity of the cover surface (0.82), σ is the Stefan-Boltzmann constant (5.67E^{-8} W/m^2 K^4), T_{ci} is the inside temperature of the cover (Equation 9), T_{sky} is the sky temperature and is given in Equation 11, k_c is the thermal conductivity of the cover, and D_{ci} is the inside diameter of the cover, D_{co} is the outside diameter of the cover, and D_r is the diameter of the receiver.

$$T_{sky} = T_a \left[0.711 + 0.0056 T_{dp} + 0.000073 T_{dp}^2 + 0.013 \cos(15t) \right]^{1/4} \quad 12$$

Where, T_{dp} is the dew point temperature and t is the hour from midnight. We chose an average dew point temperature of 26 C and an hour from midnight of 12 to put us at noon. Once Q_{loss} is found the overall heat loss coefficient can be found from Equation 13 [1].

$$U_L = \frac{Q_{loss}}{\pi D_r L * (T_r - T_a)} \quad 13$$

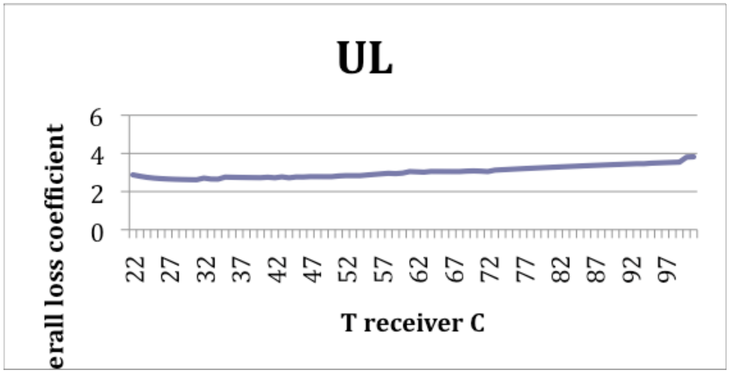

Figure 11. Shows the overall heat loss coefficient for chosen receiver/cover pipe system. Assuming no heat transfer to the supports and that the air between the receiver and cover is evacuated. For ε_c = 0.85, ε_r = 0.45, T_{dp} = 26 C, and t = 12.

Optical Performance of Receiver/Cover system

Optical performance is a key aspect of solar collection due to the fact that the system can make only make use of energy that is absorbed by the receiver pipe (also known as a heat pipe), thus the objective here is to maximize the optical performance of the receiver.

Angles

Furthermore, the orientation of the receiver tube has a huge effect due to the large variety of incident angles the sun makes with the receiver. Therefore to minimize the average angle of incidence over a year period a North-South axis and East-West tracking was chosen with a tilted trough equal to the regions latitude (32 deg in this case). The angle of incidence is given by reference [4] in Equation 14, and the solar zenith angle in equation 15.

$$\cos\theta = (\cos^2\theta_z + \cos^2\delta * \sin^2 w)^{1/2} \qquad 14$$

$$\cos\theta_z = \cos\phi * \cos\delta * \cos w + \sin\phi * \sin\delta \qquad 15$$

Where θ is the incident angle, w is the hour angle in degrees, Φ is the regions latitude in degrees, δ is the declination given by Equation 16 [1].

$$\delta = 23.45 * \sin(360 * (284 + n)/365) \qquad 16$$

Where n is the day of the year.

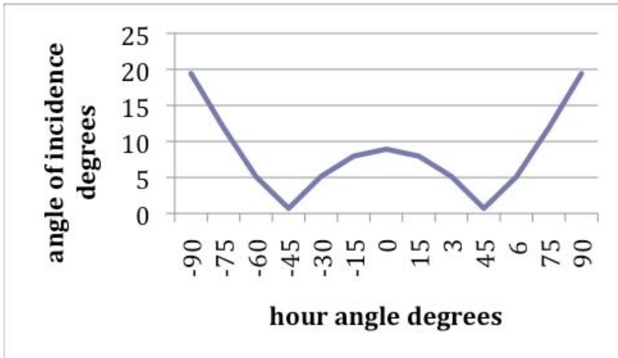

Figure 12. Incident angles for the chosen receiver pipe and orientation throughout the day. Declination = 0.4 rad = 23 degrees.

Incident Angle Modifier

Due to the fact that reflectivity, transmissivity, and absorptivity depend on the incident angle of the solar radiation, an angle modifier is needed to correct for when radiation is not normal to the surface. Incident angle modifiers are used to account for errors in solar alignment, errors in concentrating contours, and errors in displacement of receiver outside of the focal plane. These errors must be accounted for because all of these cause shifts and enlargements of the solar images, which can greatly reduce the efficiency of the system.

$$K_{DUF}(\theta) = 1 - 6.74E^{-5} * \theta^2 + 1.64E^{-6} * \theta^3 - 2.51E^{-8} * \theta^4 \qquad 17$$

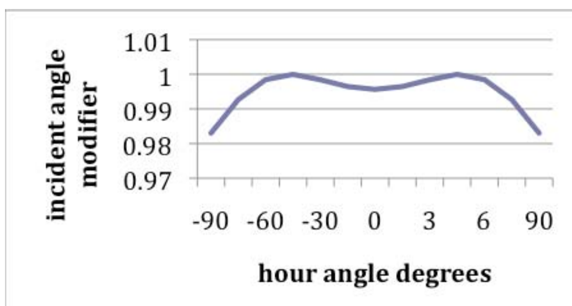

Figure 13. Incident angle modifier for chosen receiver pipe throughout the day.

Receiver Absorptivity

Absorptivity is a material property that quantifies the ability of a material to absorb radiation, in this case solar radiation. Due to fluctuations of the solar incidence an absorbtivity ratio was developed by reference [4] in equation 18.

$$\alpha / \alpha_n = 1 + 2.0345e^{-3}\theta - 1.99e^{-4}\theta^2 + 5.324e^{-6}\theta^3 * 4.799e^{-8}\theta^4 \qquad 18$$

Where α is the effective absorptivity, α_n is the normal specular absorptivity of the material itself, and θ is the angle of incidence.

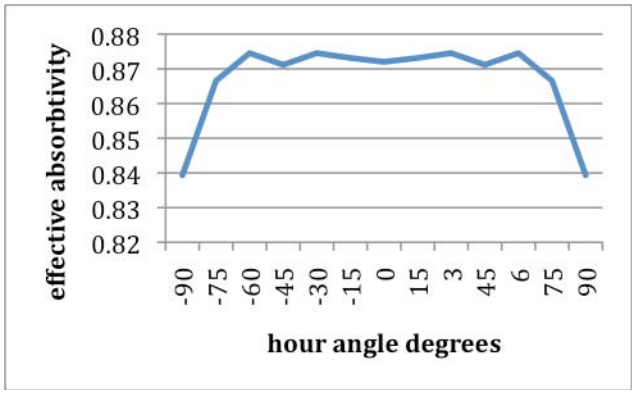

Figure 14. shows the effective absorption of solar radiation at the receiver pipe (heat pipe).

Cover system

A transparent Pyrex glass tube is sheathed concentrically around the receiver pipe to help insulate the heat pipe as well as limit re-reflection and re-radiation back to the sky. To account for the overall optical performance of the cover system the respective solar transmission, reflection, and absorption will be analyzed.

Transmission, Reflection, and Absorption

The Pyrex glass cover is assumed to have a smooth surface and thus the analysis of the amount of solar radiation transmitted through the cover needs to account for the reflection of radiation back to the sky, and the absorption of radiation by the glass sheath. The analysis for the chosen cover system is as follows.

The angle at which the solar radiation refracts when passing through the cover is given by snell's law in Equation 19.

$$n_1 / n_2 = \sin\theta_1 / \sin\theta_2 \qquad 19$$

Where, θ_1 is the incident angle of the radiation, n_1 is the index of refraction of the air ($n=1$), n_2 is the index of refraction of the glass cover, and θ_2 is angle of refraction. The un-polarized portions of the radiation passing into the glass are,

$$r_{perpindicular} = \sin^2(\theta_2 - \theta_1) / \sin^2(\theta_2 + \theta_1) \qquad 20$$

$$r_{parallel} = \tan^2(\theta_2 - \theta_1) / \tan^2(\theta_2 + \theta_1) \qquad 21$$

Thus the transmissivity of the un-polarized portions of radiation is,

$$\tau_r = \frac{1}{2} * [((1 - r_{parallel}) / (1 + r_{parallel})) + ((1 - r_{perpindicular}) / (1 + r_{perpindicular}))] \qquad 22$$

Where, τ_r is a measure of the amount of radiation transmitted with respect to what was reflected back to the sky. Now taking into account that the glass cover will absorb radiation as well, Equation 23 is used.

$$\tau_a = \exp\left(\frac{-K * L}{\cos\theta_2}\right) \quad 23$$

Where, K is the extinction coefficient (32 1/m) and is a measure of the amount of radiation that the given glass will absorb with respect to what it transmits. Equation 24 will then give the total transmissivity of the cover system.

$$\tau = \tau_a * \tau_r \quad 24$$

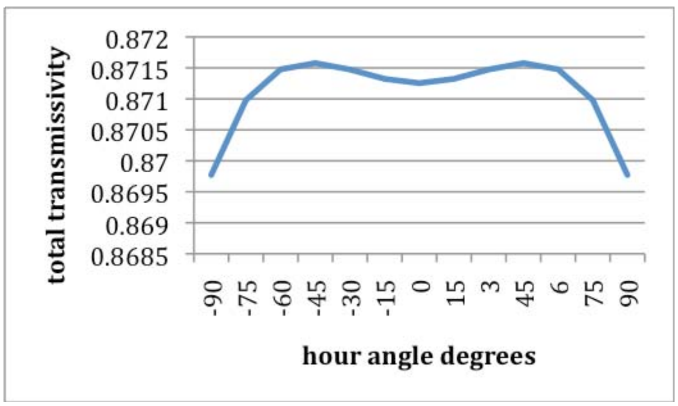

Figure 15. Total transmission of solar radiation through chosen single glazing Pyrex glass cover system. K for chosen Pyrex cover = 32 1/m.

Overall Optical Efficiency

The overall modified optical efficiency is one that accounts for the reflection of radiation from the trough, the effective specular absorptivity of the receiver, the total transmissivity of the cover, and the incident angle with tracking corrections [4].

Furthermore, reflected radiation back to the receiver must be taken into account. This is done by the intercept factor, which is the fraction of the reflected radiation that is incident on the receiver surface [4]. For a large enough diameter D_o the fraction is 1 [4]. The intercept factor was calculated as follows.

$$D_{\gamma=1} = w * \frac{\sin(0.267)}{\sin(\phi_r)} \quad 25$$

$$\gamma = \begin{cases} \dfrac{1}{D_o / D_{\gamma=1}} & \dfrac{if}{if} \; \dfrac{D_o > D_{\gamma=1}}{D_o < D_{\gamma=1}} \end{cases} \quad 26$$

Where, w is the width of the aperture, D_o is the ideal diameter for an imperfect trough (Equation 3), and φ_r is the rim angle. Now the overall modified optical efficiency can be calculated [4].

$$\eta_o(\theta) = \rho_c * \alpha * \tau * \gamma \qquad 27$$

$$\eta_{o,\text{modified}}(\theta) = K(\theta)_{DUF} * \eta_o(\theta) \qquad 28$$

Where, ρ_c is the specular reflectance of the trough, α is the effective absorptivity of the receiver surface, τ is the total transmissivity of the cover, $K(\theta)_{DUF}$ is the incidence angle modifier (Equation 17), and γ is the intercept factor.

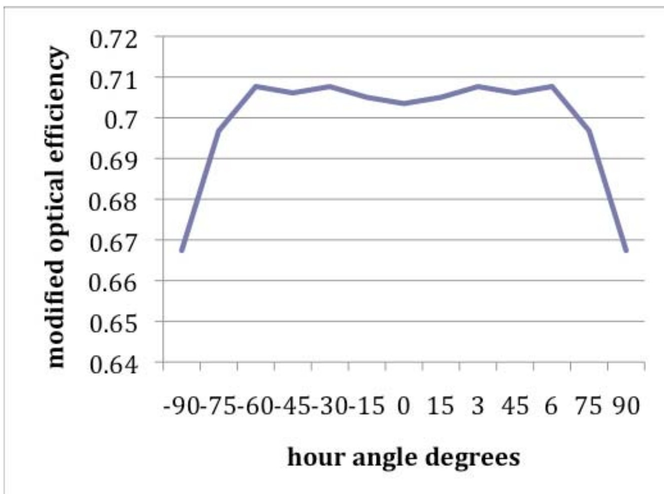

Figure 16. Overall optical efficiency of the chosen cover/receiver system throughout the day.

End Loss Coefficient

Describes the amount of radiation that is reflecting out the end of the trough, because the chosen trough is considered a short trough these effects must be accounted for.

$$\xi(\theta) = 1 - (f/L) * (1 + \frac{a^2}{48 * f^2}) * \tan(\theta) \qquad 29$$

Where, f is the focal length, L is the trough length, and a is the aperture width.

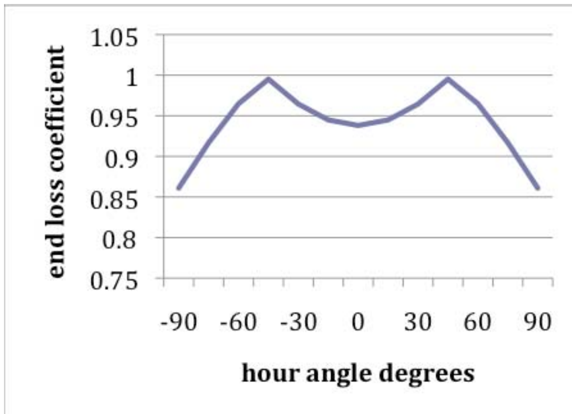

Figure 17. Effects of solar radiation losses to the sky out the ends of the chosen trough geometry.

Absorbed Radiation

With all corrections made the actual amount of radiation that is absorbed (S) by the receiver is,

$$S = I_{beam} * \eta_{o,\text{mod}}(\theta) * \xi(\theta) * \cos\theta_1 \qquad 30$$

Where, I_{beam} is the average beam solar insolation incident on the aperture is found from tables (see 'available radiation'), $\eta_{o,mod}(\theta)$ is the overall modified optical efficiency, $\xi(\theta)$ is the end loss coefficient, and θ_1 is the angle of incidence.

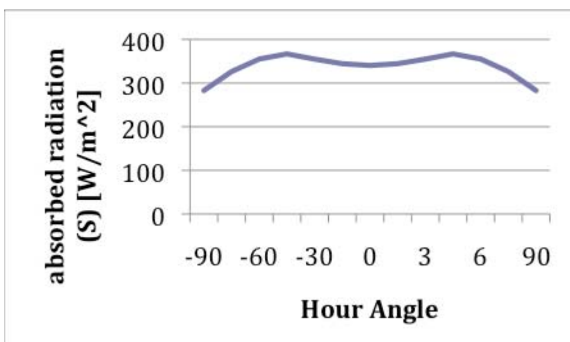

Figure 18. Overall radiation absorbed by the chosen receiver pipe throughout the day.

It follows that the average absorbed solar radiation for an average day is roughly 338.5 W/m^2.

Initial Heat Transferred to Fluid

Heat transferred to the fluid for the chosen trough length of 1.3 m. Due to the fact that the internal heat transfer is dependent on temperature, reference [4] suggests an estimated receiver temperature to evaluate the properties, see Equation 31. For the chosen receiver pipe the flow was found to be laminar (Re < 2300) at that estimated mean receiver temperature. This is because our mass flow rate is very small, only 0.007 kg/s, this is to balance the small rate of evaporation in our distiller device. Therefore, fluid properties are evaluated at,

$$T_{rm,estimate} = T_{in} + .25 * S * \frac{A_a}{C_p * \dot{m}} \qquad 31$$

And,

$$\mathrm{Re}_{fluid} = \frac{4\dot{m}}{\pi D_{ri} \mu_{fluid}} \qquad 32$$

Where, A_a is the area of the aperture ([a-D_{ro}]L), S is the absorbed radiation in watts, For turbulent flow patterns, $\dot{m}$ is the mass flow rate of the fluid in kg/s, C_p is the specific heat of the fluid. Analysis was then done for laminar flow in internal pipes.

$$Nu_{fluid} = 3.7 \qquad 33$$

The heat transfer coefficient is then found with,

$$h_{fluid} = \frac{Nu_{fluid} * k_{fluid}}{D_{ri}} \qquad 34$$

Where, k_{fluid} is the thermal conductivity of the fluid.

To account for the temperature gradients in the flow direction a collector efficiency factor and flow factor are used, and are shown below respectively [1].

$$F' = \frac{(1/U_L)}{(1/U_L) + \frac{D_{ro}}{h_{fluid} * D_{ri}} + (D_{ro}/2k_r) * \ln(\frac{D_{ro}}{D_{ri}})} \qquad 35$$

$$F'' = \frac{F_R}{F'} = \frac{\dot{m}C_p}{A_r U_L F'}\left[1 - \exp(-\frac{A_r U_L F'}{\dot{m}C_p})\right] \qquad 36$$

Where, C_p is the specific heat of the fluid, A_r is the receiver area ($\pi D_{ro}L$), and U_L is the overall loss coefficient. Now the useful energy gain, mean fluid and receiver temperatures for the chosen trough can be calculated as follows,

$$Q_{useful} = F_R A_a \left[S - \frac{A_r}{A_a} U_L * (T_{in} - T_a) \right] \qquad 37$$

$$T_{rm} = T_{in} + \frac{Q_{useful} / A_r}{F_R * U_L} * (1 - F_R) \qquad 38$$

$$T_{fm} = T_{in} + \frac{Q_{useful} / A_r}{F_R * U_L} * (1 - F") \qquad 39$$

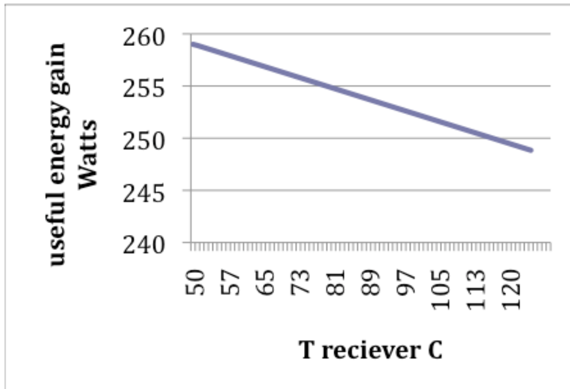

Figure 19. Useful energy gain as a function of receiver temperature for the chosen receiver pipe.

Heating the Water to Saturation Temperature

For the purposes of this project the objective is to heat the water to saturation temperature, because we want to maximize water vapor production. Therefore for this analysis the useful energy gain per meter was calculated, in order to establish an approximate length to vaporization. So, in this situation we know the inlet temperature of the fluid and the saturation temperature of water, thus these will be our inlet and outlet temperatures. The saturation temperature is dependent on pressure at the inlet, here it is assumed that atmospheric pressure exists and T_{sat}=100 C.

However, because these temperatures cause a gradient in the flow direction the flow patterns inside the pipe can be laminar and/or turbulent. Heat transfer increases significantly in turbulent flow than laminar flow [4]. This is accounted for by evaluating the Reynolds number at the inlet and outlet of the receiver pipe. If both are found to be laminar then laminar heat transfer correlations can be used, visa versa if both are found to be turbulent. However, if the pipe exhibits flow patterns that are both laminar and turbulent, as it is for the chosen receiver pipe, reference [4] suggests estimating an average heat transfer correlation using average Re and Pr numbers, as follows in Equation 41.

$$\mathrm{Re}_{fluid} = \frac{4\dot{m}}{\pi * D_{ri} * \mu_{fluid}} \qquad 40$$

$$Nu_{average} = 3.7 * \frac{Re_{2300} - Re_{in}}{Re_{sat}} + \frac{Re_{sat} - Re_{2300}}{Re_{sat} - Re_{in}} * \frac{(f/8) * Re_{turb,ave} * Pr_{turb,ave}}{1.07 + 12.7 * \sqrt{(f/8)} * (Pr_{turb,ave}^{2/3} - 1)} * (\mu_{fluid} / \mu_w)^{.11} \quad 41$$

$$f = (0.79 * \ln(Re_{turb,ave} - 1.64))^{-2} \quad 42$$

Where,

$$Re_{turb,ave} = (\frac{Re_{2300} + Re_{sat}}{2}) \quad 43$$

$$Pr_{turb,ave} = (\frac{Pr_{2300} + Pr_{sat}}{2}) \quad 44$$

$$Re_{2300} = 2300 \quad 45$$

Re_{in} is the Reynolds number evaluated at the inlet temperature of the receiver pipe, Re_{sat} is the Reynolds number evaluated at the saturation temperature, $\dot{m}$ is the mass flow rate of the fluid, μ_{fluid} is the kinematic viscosity of the fluid, and μ_w is the kinematic viscosity of water.

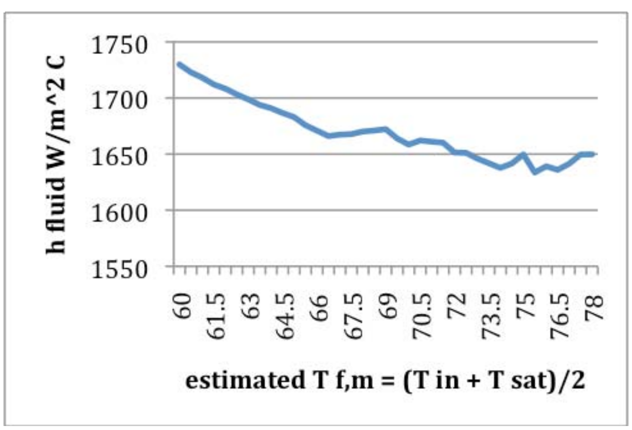

Figure 20. Shows the heat transfer coefficient of the fluid inside the receiver pipe as a function of T for the chosen receiver tube and mass flow of 0.007 kg/s.

In order to evaluate a length to heat water to saturation, reference [4] suggests evaluating the useful gain per unit length.

$$q'_{useful} = F' * \frac{A_a}{L} * (S - \frac{A_r}{A_a} * U_L * (T_f - T_a)) \quad 46$$

Where, F' is the efficiency factor (Equation 35), L is the trough length, A_r is the receiver area ($\pi D_{ro} L$), and T_f is the mean fluid temperature as shown in Equation 47. Furthermore, Properties are evaluated at this estimated mean fluid temperature as well [4].

$$T_{fm} = \frac{(T_{in} + T_{sat})}{2} \quad 47$$

Where, T_{in} is the inlet temperature of the fluid and T_{sat} is the saturation temperature of the fluid at the inlet pressure. From the above the mean receiver temperature can be found in Equations 48 [4].

$$T_{rm} = T_{fm} + q'_{useful} * (\frac{1}{h_f} + \frac{\ln(D_{ro}/D_{ri})}{2\pi k}) \quad 48$$

The length to heat the fluid to saturation temperature is given by reference [4] as follows,

$$L_{sat} = (T_{sat} - T_{in}) * \frac{C_p * \dot{m}}{q'_{useful}} \quad 49$$

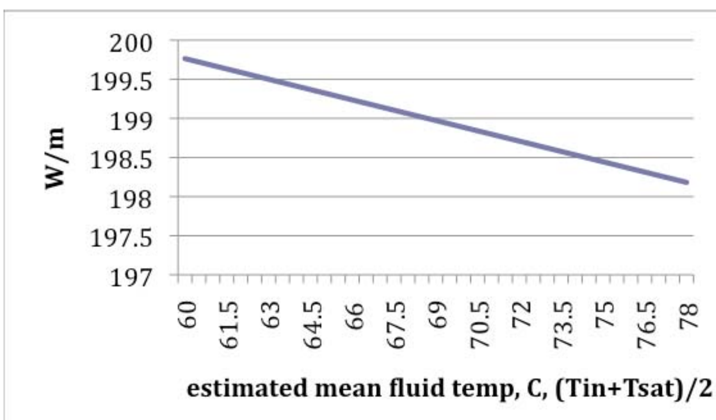

Figure 21. Average useful gain per meter of the chosen receiver pipe as a function of fluid temperature.

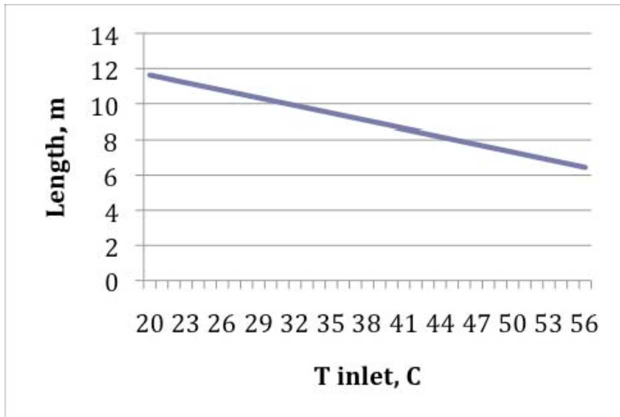

Figure 22. Estimated length to heat water to the saturation temperature for the chosen receiver pipe as a function of inlet temperature. T_{sat} =100 C, because atmospheric pressure is assumed at the inlet of the receiver pipe. Note: calculation done for horizontal axis system.

Due to the fact that our chosen design is only 1.3 m in length the water will be cycled through the same receiver tube multiple times (these will be referred to as passes) as the receiver gets hotter throughout the day. Therefore, if the receiver tube is 1.3 m and our flow rate is 0.007 kg/s of water then the average free stream velocity can be calculated from the average density of water, thus V = 0.0466 m/s. Then it takes the water 86 s to complete one pass through the receiver pipe. If the water has to travel approximately 3.5 m to return to the inlet of the receiver pipe it takes another 75 s to do so, thus, a total of 161 s to complete on pass. The total number of passes needed can be found by the ratio L_{sat}/L and as a result the time it will take to heat the water to T_{sat} can be estimated as 161 s * L_{sat}/L = 25 minutes.

Moreover, there will be some heat losses by cycling the water through the system this way that have not been taken into account to this point in the design process.

Cross Section Temperature Profile of the Receiver Pipe

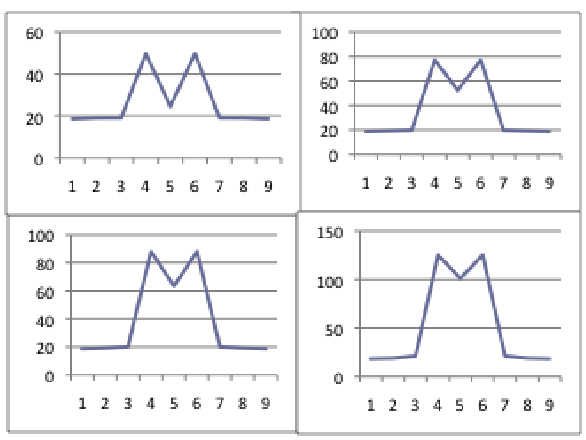

Figure 23. Shows the temperature distribution of the entire absorber pipe (receiver and cover) in the radial direction in degrees C. The circles depict the absorber pipe cross section. Temperature at 1 and 9 is T_{sky}, temperature at 2 and 8 is T_a, temperature at 3 and 7 is T_{cover}, temperature at 4 and 6 is $T_{receiver}$, and the temperature at 5 is T_{fluid}. All for the chosen receiver pipe and trough system.

Determining Distiller Geometry

The incoming heat to the distiller is added from the solar trough collection system which adds approximatly 250 useful W to the fluid each pass the fluid makes.

Thus the temperature of the water that pools, where most of the evaporation takes place, in the distiller are estimated to be the mean outlet temperature of the receiver pipe through out the cycle to get the water heated to saturation temperature (mean outlet temperature ranges from about 30 – 120 C).

Calculations (done at steady state) of the heat transferred inside the distiller, the mass flux inside the distiller, and the condensation rate inside the distiller were all analyzed as a function of distiller area, in order to determine an acceptable distiller geometry. Taking all these into account will allow the maximization of surface area for evaporation and the minimization of surface area for heat losses.

Initially, the following equations for free convective heat transfer were calculated as a function of distiller diameter ($D_{distiller}$). In order to evaluate the heat transfer in various distiller sizes. The thermal properties of air were evaluated at T_{eval}.

$$T_{eval} = \frac{T_{m,o} + T_{\infty}}{2} \tag{50}$$

$$Ra = \frac{g\beta * (T_s - T_{\infty}) D_{distiller}{}^{3}}{\nu\alpha} \tag{51}$$

Where,

$$\beta = \frac{1}{T_{abs}} \tag{52}$$

T_s is estimated as the mean outlet temperature of the reciever heat pipe, T_{∞} is the temperature of the top surface of the distiller, which is unknown initially and thus, estimated as the temperature of the incoming heat exchange fluid (30 C).

The heat transfer due to free convection in the distiller is then,

$$N\overline{u} = .15 Ra^{1/3} \tag{53}$$

$$\overline{h} = \frac{N\overline{u} * k_{air}}{D_{distiller}} \tag{54}$$

Applying the mass transfer analogy the average mass transfer coefficient can be calculated and ultimatley the mass flux.

$$\frac{h}{h_m} = \frac{k}{D_{AB} Le^{1/3}} \quad 55$$

Where,

$$Le = \alpha / D_{AB} \quad 56$$

α is the diffusivity of air, k is the thermal conductivity of air, and D_{AB} is the diffusion coefficient of air. The average mass flux in kg/m^2 s is,

$$N" = \bar{h}_m * (C_{A,s} - C_{A,\infty}) * \mathrm{M}_{water} \quad 57$$

Where,

$$C_{A,s} = \frac{p_{sat}(T_s)}{RT_s} \quad 58$$

$$C_{A,\infty} = C_{A,s} * \Theta_{rel} \quad 59$$

$$\mathrm{M}_{water} = 18 kg/kmol \quad 60$$

$p_{sat}(T_s)$ is the saturation pressure at the mean outlet temperature of the receiver pipe, R is the universal gas constant (8.314 J/K mol), Θ_{rel} is the relative humidity (estimated to be 70%), and here T_s is the evaporate pool mean temperature estimated at $T_{\text{mean outlet receiver pipe}}$.

The average mass flux was then analyzed as a function of distiller area.

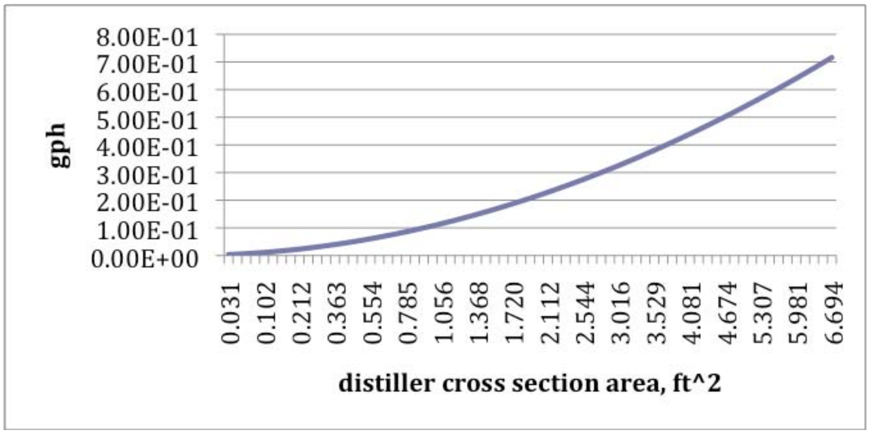

Figure 24. Average gallons per hour of mass (water vapor) leaving the evaporate pool as a function of distiller area for the chosen system.

The overall average heat transfer inside the distiller is a combination of the free convective heat transfer and the heat transferred by evaporation. Therefore,

$$Q''_{conv} = \bar{h} * (T_s - T_\infty) \qquad 61$$

$$Q''_{evap} = N''*H_{fg} \qquad 62$$

Where, N" is the mass per unit area leaving the surface and H_{fg} is the heat of vaporization of water in j/kg, T_s is the temperature of the fluid inside the distiller, and T_∞ is the temperature of the top surface and is initially unknown. However, the top surface temperature needs to be maintained at a temperature that will maximize condensation and yet maximize heat transferred to the cool heat exchange fluid, this temperature is designed to be 29-30 C for the chosen geometry; this analysis is done in the 'heat exchanger' section.

The average heat transferred to the top surface is then,

$$Q''_{ave} = Q''_{conv} - Q''_{evap} \qquad 63$$

From this thermal analysis the following results were calculated.

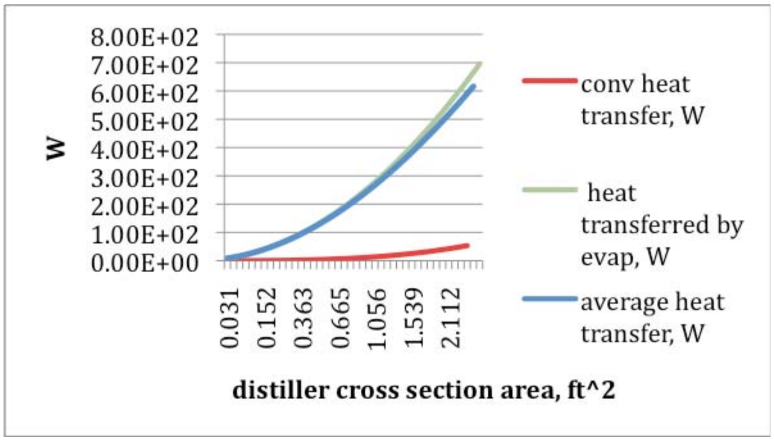

Figure 25. Summarizes the heat transferred from the evaporate pool to the top surface due to free convection and evaporation effects as a function of distiller area for the chosen system.

With the heat transferred to the top surface, the rate of condensation in [kg/m^2 s] on that surface can be estimated as follows.

$$\dot{m}_{condensation} = \frac{Q_{evap}}{h'_{fg}} \quad 64$$

Where,

$$h'_{fg} = H_{fg} + .68 * C_p (T_{sat} - T_s) \quad 65$$

C_p is the specific heat of the water in the distiller and T_s is the temperature of the top surface of the distiller.

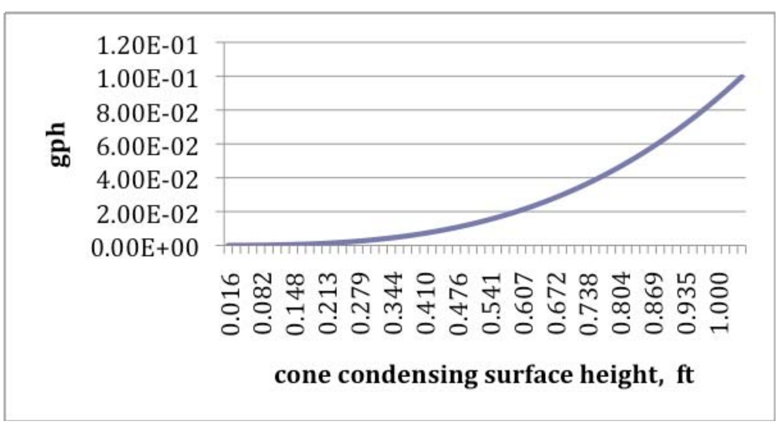

Figure 26. Shows the average rate of condensation as a function of condensing surface area for the chosen system.

From the data calculated above a distiller size was chosen. A cross sectional surface area of approxomatly 2.5 ft^2 with a height of 6 in was chosen. As for the condensing surface a height of 1 foot was chosen to maximize condensation rates.

Heat Exchanger

The hot condensate from the hot evaporation pool will transfer heat to the the cool condensing surface, which is why the surface must be continually cooled by a heat exchanger. want to keep top surface temp at 29 C the condensate raises the temp of the surface and to keep the surface temp at 29 C to allow for an ideal condensation rate for the chosen geometry.

In order for the temperature of the condensing surface to stay reletivley mild the delta T of the cool heat exchange fluid needs to be equal to the amount of heat to be extrated from the surface, that is being heated by the condensate. The cahnge in temperature of the heat exchange fluid will represent heat being lost from the surface and added to the heat exchange fluid, thus for the following analysis a mass flow rate of the heat exchange fluid was calculated to maximize the transfer of heat to the fluid and thus from the surface.

The heat transfer to the surface by the condensate is estimated with laminar film stream flowing down a vertical plate correlations, therefore,

$$\bar{h}_{condensate} = 0.943 * \left(\frac{g * [(1/\nu_l) - (1/\nu_v)] * k_l^3 * h'_{fg}}{\mu_l * (T_{sat} - T_s) * L}\right) \quad 66$$

$$\Delta T_{topsurface} = \frac{Q_{evap}}{\bar{h}_{condensate}} \quad 67$$

Where, ν_l is the specific volume of the liquid water, ν_v is the specific volume of the water vapor, k_l is the thermal conductivity of the liquid water, μ_l is the kinematic viscosity of the liquid water, T_s is the top condensing surface temperature, and L is the height of the cone top condensing surface.

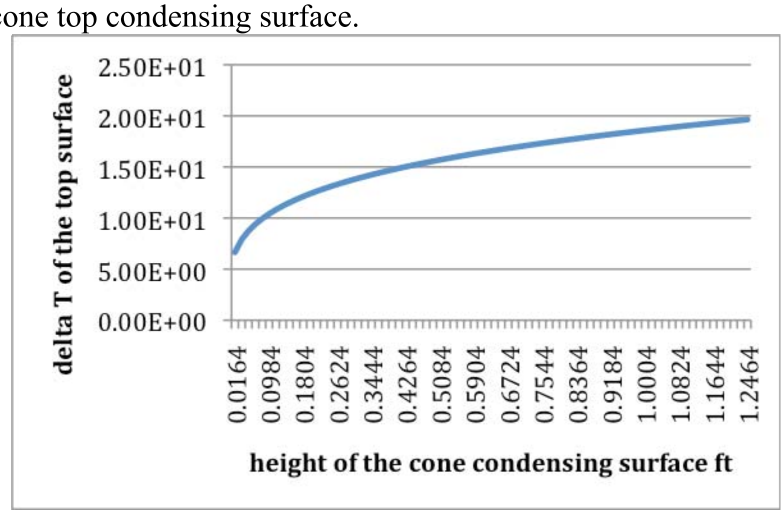

Figure 27. Shows the delta T of the top condensing surface due to the heating effects from the condensation process as a function of the condensing surface geometry.

A delta T of 40 C was chosen. Since the temperature of the fluid is raised 40 C that approximatly represents a loss of 40 C from the surface, thus cooling the surface so additional condensation can occur.

Heat transfer coefficient was estimated to be 600 W/m^2 K, as suggested by reference [6] for water vapor to water heat transfer through a stainless steel surface. The energy transferred to the fluid is described in Equation 68.

$$Q = \dot{m} C_p \Delta T \quad (68)$$

Where, Q is estimated as the amount of heat transferred to the top condensing surface via convection and evaporation, $\dot{m}$ is the mass flow rate of the heat exchange fluid, and ΔT is 40 C.

Therefore a mass flow rate of 0.0173 kg/s is needed to balance the temperature of the surface to about 30 C.

Results

Flow rate of heat exchange fluid to cool condensing surface	Distiller cross sectional area	Distiller height	Cone shaped condensing surface height	Estimated time to heat water to saturation temperature at steady state	Estimated useful energy gain of solar energy to fluid per pass
0.0173 kg/s	**2.5 ft^2**	**6 in**	**1 ft**	**25 min**	**260 W**
Average condensation rate	**Average daily insolation used for calculations in San Diego**	**Average mass flux**	**Average Mass Flow Rate inside receiver pipe**		
0.008-0.1 gph	**522 W/m^2**	**0.2-0.35 gph**	**0.007 kg/s**		

Conclusions and Recommendations

In regards to our solar water distillation concept, our team has come to conclusion of an overall design and concept of our final assembly. The enhanced solar water trough has undergone several iterations to produce maximum potable water production. The overall basic geometry of the solar water distillation comprises of:

- 32 degree applied tilted angle silver acrylic film tape trough
- Absorber tube (Pyrex® glass cover and copper heated pipe)
- Spray nozzle
- Distiller with heat exchanger
- Integrated piping with insulation

- Bachmann mini water pump
- Distilled water reservoir

These key components of our application with allow for contaminated water input and clean drinkable water output through condensate distillation. Therefore, the user is able to produce drinkable water priceless through our invention. This is engineered through a dynamic process of solar energy, evaporation, and condensation. The procedure is accomplished as follows:

- Contaminated water enters an absorber tube (Pyrex glass cover, copper heat pipe) oriented at the focus of a parabolic reflective trough.
- Heated water exits absorber tube and enters distiller via spray nozzle to increase surface area per droplet to enhance evaporation.
- Remaining hot water pools and distiller then allows for further evaporation.
- Vapor is condensed on a cooled condensing surface via heat exchanger oriented on the top of the distiller
- Heat exchanger uses cool contaminated water flow to cool the condensing surface and preheat the incoming water
- Condensed potable water drains out of distiller via gravity into a collection tube

Our six-point system allows for the production of 2-3 gallons of purified water daily within ideal solar conditions. The primary goal for our project is to accommodate our user with nourished water without the need of traveling. Also, 3rd world countries will be safer and healthier with the simple use of our solar water distillation application.

Comparison with Existing Designs

Water cone: The water cone invented by Stephan Augstin, is a simple distiller that is similar to our distiller in a lot of ways. The conical shaped design allows for the process of solar distillation. The top of the water cone has a screw cap spout which allows for the collection of the clean water. In comparison with the water cone, our parabolic solar water distiller is fixed and automatically collects the purified water without the labor or rotating the entire device upside down like the water cone seen in the figure below.

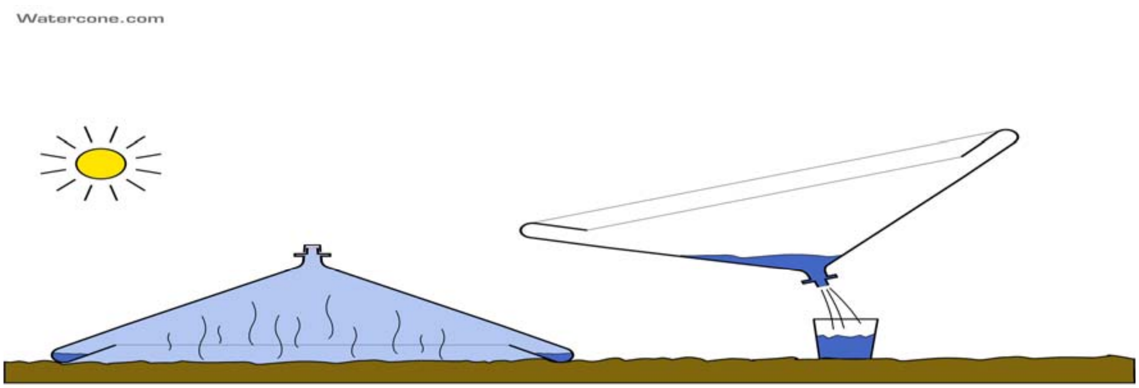

Figure 28. Water Cone applying condensation via V-shaped collector.

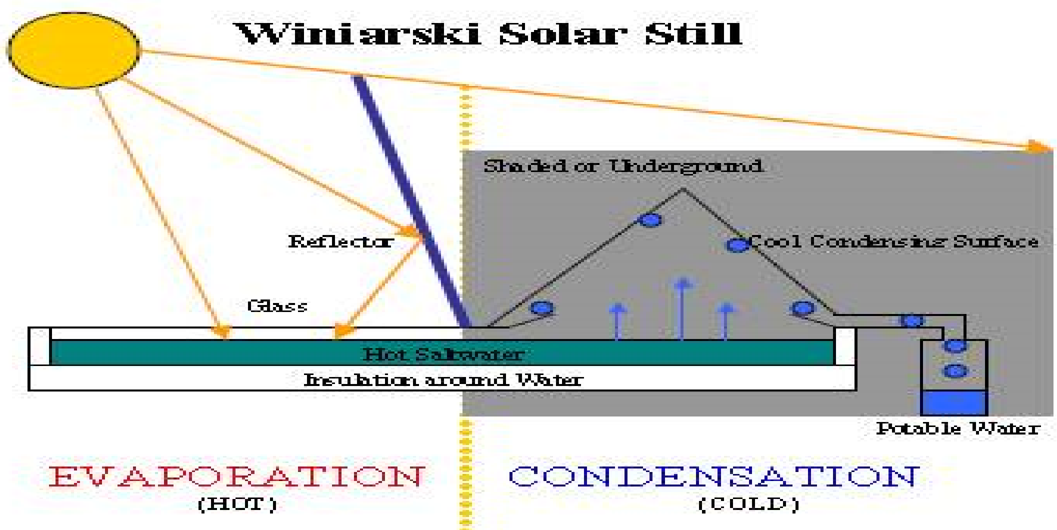

Figure 29. Winiarski Solar Still applying condensation via V-shaped collector.

Florida Solar Energy Center: This device uses a parabolic trough to concentrate solar energy on a copper pipe just. The copper pipe uses the heat exchange principle similar to ours except that our heat exchanger is coupled with the distiller. The untreated water is then pumped into the outer channel, where it is heated directly by the concentrated solar energy. After the water reaches the end of the pipe, it returns through the middle channel, and preheats the untreated water. Preheat is idle for the Florida Solar energy project yet the conditions for our parabolic solar distillation do not require preheating. In comparison, photovoltaic panel supplies electricity for the pump for both our application and theirs. Experiments at the Florida Solar Energy Center showed that this device would produce up to 660 gallons of drinking water per day, using a 92-square-foot concentrator. The developers have estimated that the cost of materials for this device is about $1,680. When the cost of the pump and reservoirs is added, this becomes one of the more expensive devices. Our parabolic solar water distillation project will not produce as much gallons of drinking water per day therefore cost of materials will be substantially cheaper.

Learning Experience

Our parabolic solar water distillation project allowed our team to interface with mechanical engineering problematic circumstances. Project goals induced our group into planning and engaging in systematic approaches for project management and design. Some important learning aspects for our "real world" project included:

- Effective time and team management
- Applying conceptual design methods
- Intertwine science, mathematics, and engineering
- Use techniques, skills, and tools for engineering practices
- Ability to identify, formulate, and solve engineering problems

The project introduced our team into a learning environment within several important areas of mathematics and science. Specializing and engaging into the monumental development of solar applications, we were able to apply our knowledge to furthermore help the expansion of solar green movement. Therefore, our parabolic solar water distillation application integrated the research development within the following areas:

- Solar Energy
- Chemistry
- Fluid Dynamics

These three areas were crucial for our application emphasizing on solar energy. Our world has historically overtaxed its resources, but by solar energy, we could perhaps give back what it gave to us by improving our energy efficiency. The parabolic solar water distillation will improve solar energy efficiency and accommodate the user with an efficient water source.

Future Research and Development

After a semester of research and calculations, we have settled on a final design of a solar still, a solar still that will maximize potable water production. Some of our future research and development consist of:

- Refinement and consistency improvements
- Receiving a constant film flow of water down the coned heat transfer surface
- Spray nozzle at heat exchanger inlet
- Fabric material or grooves to distribute the water over the surface
- Fabrication and assembly of our design
- Prototype testing/data acquisition

Strengths and Weaknesses

The objective of this system is to heat water to vaporization, and not to produce high quality steam. Taking into account thermal performance, heat loss, absorptivity, and all other variables, we were able to pinpoint our condensation rate at .5 (gph) for our solar distiller. Optimum optical efficiency at .71 and absorbed radiation at 338.5 W/m^2 followed as well. Overall, we might have to maximize the distiller geometry volume to allow for utmost condensation.

Acknowledgements

Sponsor: Akasha Kaur Khalsa

Advisor: Dr. Fletcher Miller

Special Thanks: Dr. Kee Moon

References & Works Cited

[1] Duffie, J & Beckman, W. Solar Engineering of Thermal Processes. Wiley. 3rd ed. 2006.

[2] Akasha Kaur Khalsa & DeAndre, D. “Thermal Reflectivity in Solar Collector Prototype”. Senior Design Project. 2008.

[3] National Renewable Energy Laboratory. (2010, April 28). Redbook. http://rredc.nrel.gov/solar/old_data/nsrdb/redbook/sum2/23188.txt

[4] Jacobson, E & Ketjoy, N. Solar Parabolic Trough Simulation and Application for a Hybrid Power Plant in Thailand. niponk@nu.ac.th

[5] Archer, D. Qu, M & Masson, S. (2006). Renewable Energy Resources and a Greener Future. “A Linear Parabolic Trough Solar Collector Performance Model”. Vol 8.

[6] Engineering Toolbox. (2010, April 29). http://www.engineeringtoolbox.com/overall-heat-transfer-coefficients-d_284.html

Augstin, Stephan. Water Cone Website. (2010) Available www.watercone.com /product.html

Rolla, Trudy. (1998) “Sun and water: an overview of solar water treatment devices.” Available www.solarcooking.org/sunandwater.htm

“Aprovecho Research.” (2010) www.aprovecho.net

"Water Facts." Water.org: Learn about the Water Crisis. 26 April 2010. http://water.org/learn-about-the-water-crisis/facts/

Worm, Kally. "Groundwater Drawdown." Water is Life. 29 March 2010. 27 April 2010. <http://academic.evergreen.edu/g/grossmaz/WORMKA/>.

"Progress on Drinking Water and Sanitation: Special focus on Sanitation." unifec.org. 2008. 28 April 2010. <http://www.unicef.org/media/files/Joint_Monitoring_Report_-_17_July_2008.pdf>.

Oliver, Rachel. "All About: Water and Health." CNN.com/Asia. 18 December 2007. 24 April 2010. <http://edition.cnn.com/2007/WORLD/asiapcf/12/17/eco.about.water/>.

"Patent Searching Database." freepatentsonline: all the inventions of mankind. April/May 2010. <http://www.freepatentsonline.com/search.html>.

Telkes, Maria. "Fresh Water from Sea Water by Solar Distillation." ACS Publications. May 1953. 25 April 2010. <http://pubs.acs.org/doi/abs/10.1021/ie50521a062 >.

Scrivani, El Asmar, and Bardi. "Solar trough concentration for fresh water production and waste water treatment." EuroMed 2006: Conference on Desalination Strategies in South Mediterranean Countries. 5 February 2010.

Rolla, Trudy. "Sun and water: an overview of solar water treatment devices." Journal of Environmental Health. May 1998. 23 April 2010. <http://solarcooking.org/sunandwater.htm>.

Brooks, Mills, & Harms. "Performance of a parabolic trough solar collector." Journal of Energy in Southern Africa. Vol 17 No. 3. August 2006.

Xiao, Gang. "Manual making of a parabolic solar collector." Université de Nice. 2007. April 23 2010. <http://wims.unice.fr/xiao/solar/diy-en.pdf>.

Kearney, Dr. David W. "Parabolic Trough Collector Overview." NREL Parabolic Trough Workshop. March 2007.

Kennedy, C.E. "Review of Mid- to High-Temperature Solar Selective Absorber Materials." Technical Paper sponsored by NREL, U.S. Dept. of Energy. July 2002. 9 April 2010. <http://www.osti.gov/bridge/product.biblio.jsp?query_id=0&page=0&osti_id=15000706 >

Appendix A
Literature Review

US005632823A

United States Patent [19]

Sharan

[11] **Patent Number:** **5,632,823**

[45] **Date of Patent:** **May 27, 1997**

[54] **SOLAR TRACKING SYSTEM**

[76] Inventor: **Anand M. Sharan**, 67, Ennis Ave., St-John's, Newfoundland, Canada, A1A 1Y7

[21] Appl. No.: **593,468**

[22] Filed: **Jan. 29, 1996**

[51] **Int. Cl.^{6}** **H01L 31/042**

[52] **U.S. Cl.** **136/246**; 250/203.4; 353/3; 126/602; 126/603; 126/605; 126/608

[58] **Field of Search** 136/246; 353/3; 250/203.4; 126/575–576, 602–603, 605–608

[56] **References Cited**

U.S. PATENT DOCUMENTS

3,070,699	12/1962	Lehmann et al.	136/246
4,172,739	10/1979	Tassen	136/246
4,440,150	4/1984	Kaehler	126/602
4,476,853	10/1984	Arbogast	126/578
4,628,142	12/1986	Hashizume	136/246
4,832,001	5/1989	Baer	126/579

Primary Examiner—Aaron Weisstuch

[57] **ABSTRACT**

The solar tracking system maintains a solar collector with its responsive surface normal to the sun rays. It includes a shaft supported for rotation about an axis parallel to the north-south axis of the earth, a stepper motor for intermittent rotation of the shaft at a mean rate equal to the earth's rate of rotation. A solar collector securing assembly is located on one side of the shaft and includes a bracket, collars securing the bracket to the shaft, a support for fixing a solar collector pivoted to the bracket about a pivotal axis transverse to the shaft to vary the inclination of the support relative to the shaft and stays between the support and the bracket to maintain the support at an adjusted inclination. A counter-balancing system includes an arm secured to the shaft and extending normal thereto and away from the assembly and a weight adjustably mounted on the shaft. This system counter-balances the assembly and a solar collector fixed thereto irrespective of the rotational position of the assembly about the shaft and the inclination of the support relative to the shaft. Preferably, two solar collectors are mounted on the shaft, one being an array of solar cells feeding a battery which in turn feeds a stepper motor driving the shaft through a step down gear box. The sun shadow of a pointer normal to the solar collector panel serves to properly align the panel. Alternately, the current generated by the solar cells is measured and its maximum indicates that the solar panel is properly aligned with the sun.

14 Claims, 4 Drawing Sheets

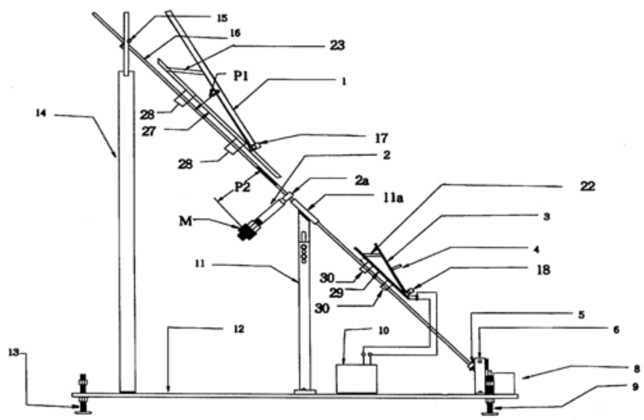

Figure 30. Solar Tracking System.

US 20080029150A1

(19) United States

(12) Patent Application Publication (10) Pub. No.: US 2008/0029150 A1

Quero et al. (43) Pub. Date: Feb. 7, 2008

(54) SOLAR CONCENTRATOR PLANT

(75) Inventors: **Valerio Fernandez Quero**, Sevilla (ES); **Marcelino Sanchez Gonzalez**, Alcorcon-Madrid (ES); **Rafael Osuna Gonzalez-Aguilar**, Sevilla (ES)

Correspondence Address:
LAW OFFICE OF JOHN C. MCMAHON
P.O. BOX 30069
KANSAS CITY, MO 64112

(73) Assignee: **Solucar, Investigacion y Desarrollo, (Solucar R & D), S.A.**, Sevilla (ES)

(21) Appl. No.: **11/729,336**

(22) Filed: **Mar. 28, 2007**

(30) **Foreign Application Priority Data**

Aug. 4, 2006 (ES) 200602134

Publication Classification

(51) **Int. Cl.**
H01L 31/042 (2006.01)

(52) **U.S. Cl.** **136/248**

(57) **ABSTRACT**

Which, using a heat transfer fluid in any thermodynamic cycle or system for using process heat, comprises:

two-dimensional solar concentrator means for heating the heat transfer fluid from a temperature T**1** to a temperature T**2**;

three-dimensional solar concentrator means for overheating the heat transfer fluid from a temperature T**2** to a temperature T**3**;

such that the advantages of working at high-temperatures of the three-dimensional solar concentrator means are taken advantage of with overall costs similar to those of two-dimensional solar concentrator means.

In a specific application for generating electric power, the two-dimensional solar concentrator means consist of a parabolic trough collector (**1**), while the three-dimensional solar concentrator means consist of a heliostat field and central tower (**2**) for generating overheated steam that expands in a turbine (**6**) coupled to an electric generator (**7**).

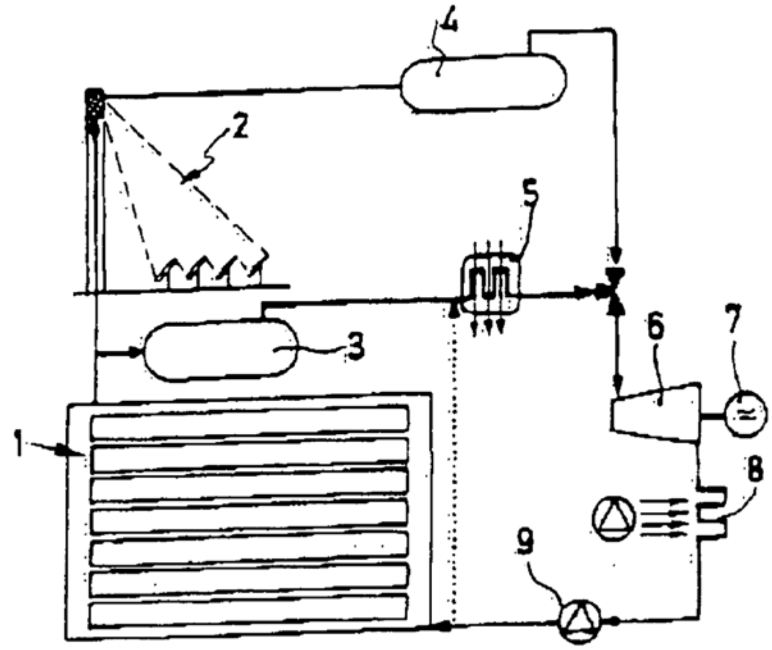

Method for Estimating Light Reflectance

US 20090316156A1

(19) **United States**

(12) **Patent Application Publication** (10) **Pub. No.: US 2009/0316156 A1**

Takagi (43) **Pub. Date: Dec. 24, 2009**

(54) **METHOD FOR ESTIMATING REFLECTANCE**

(76) Inventor: **Atsushi Takagi**, Aichi-ken (JP)

Correspondence Address:
FINNEGAN, HENDERSON, FARABOW, GARRETT & DUNNER LLP
901 NEW YORK AVENUE, NW
WASHINGTON, DC 20001-4413 (US)

(21) Appl. No.: **12/373,942**

(22) PCT Filed: **Jul. 23, 2007**

(86) PCT No.: **PCT/JP2007/064415**

§ 371 (c)(1), (2), (4) Date: **Jan. 15, 2009**

(30) **Foreign Application Priority Data**

Jul. 21, 2006 (JP) 2006-199067

Publication Classification

(51) **Int. Cl.**
G01N 21/55 (2006.01)

(52) **U.S. Cl.** **356/445**

(57) **ABSTRACT**

A reflectance of a color shifted painting color is also measured conveniently.

A first reflectance $R(\alpha_a)$ of a first reflected light V_a inside an incident plane A is measured, and a first locus l of termini of first bisection vectors $H_a(|H_a|=|R(\alpha_a)|)$, which displaces two-dimensionally inside the incident plane A, is determined. A second reflectance $R(\alpha_b)$ of a second reflected light V_b outside the incident plane A is measured, and a second locus m of termini of second bisection vectors H_b $(|H_b|=|R(\alpha_b)|)$, which displaces three-dimensionally outside the incident plane A, is measured. A locus n (x, y, z_i) of a terminus of a bisection vector H_i on a plane z=z that is parallel to a plane under measurement is approximately modeled with a numerical equation showing an ellipse from the first locus l and the second locus m, thereby determining an approximation model equation, and an overall locus n'(x, y, z) of the overall termini of bisection vectors H' of reflected lights V' other than the first reflected light V_a and the second reflected light V_b is approximately determined.

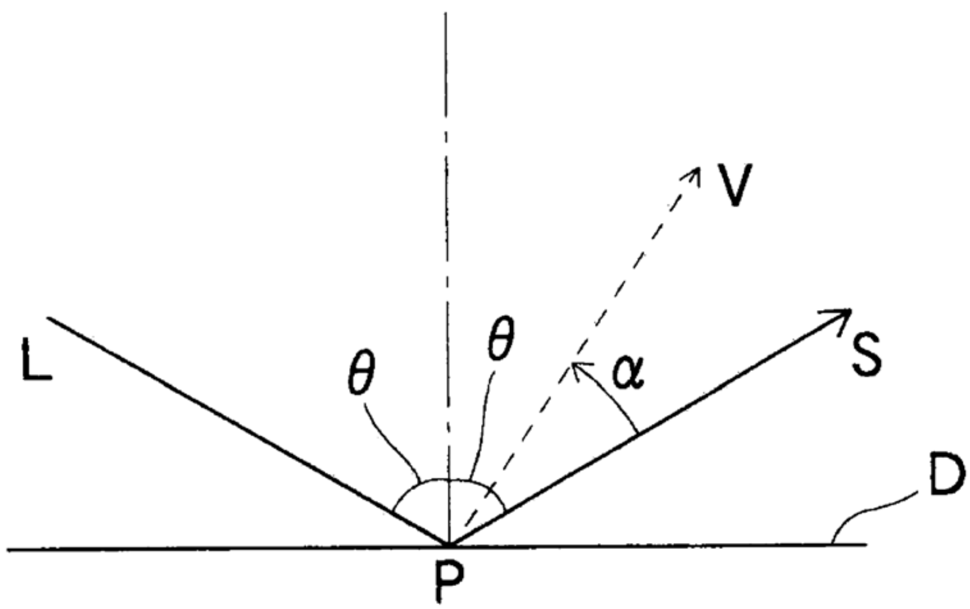

Solar Collection System Utilizing a Collapsing Trough Design

(12) **United States Patent** (10) **Patent No.: US 6,363,928 B1**
Anderson, Jr. (45) **Date of Patent: Apr. 2, 2002**

(54) **SOLAR COLLECTION SYSTEM**

(75) Inventor: **James D. Anderson, Jr.**, Pensacola, FL (US)

(73) Assignee: **Alternative Energy Group, Inc.**, Pensacola, FL (US)

(*) Notice: Subject to any disclaimer, the term of this patent is extended or adjusted under 35 U.S.C. 154(b) by 0 days.

(21) Appl. No.: **09/543,386**

(22) Filed: **Apr. 4, 2000**

(51) **Int. Cl.**[7] **F24J 2/38**

(52) **U.S. Cl.** **126/577**; 126/578; 126/573; 126/604; 126/605; 126/606

(58) **Field of Search** 126/578, 574, 126/601, 600, 605, 606, 573, 576, 577, 604, 684, 692, 696; 250/203.4

(56) **References Cited**

U.S. PATENT DOCUMENTS

3,613,659 A		10/1971	Phillips	....	126/270
4,068,653 A	*	1/1978	Bourdon et al.	....	126/271
4,134,387 A		1/1979	Tornstrom	....	126/270
4,136,671 A		1/1979	Whiteford	....	126/271
4,138,994 A	*	2/1979	Shipley, Jr.	....	126/271
4,146,785 A	*	3/1979	Neale		

(List continued on next page.)

Primary Examiner—Carl D. Price
(74) *Attorney, Agent, or Firm*—Robert C. Kain, Jr.; Fleit, Kain

(57) **ABSTRACT**

The solar tracking mechanism is utilized in connection with a solar energy collection system. The collection system includes a light reflective shell shaped to focus solar radiation on a radiation absorbing segment of a tube which carries a heat transfer fluid. The shell is pivotally mounted on a support frame. An actuator mounted between the support frame and the shell rotatably the shell. A solar sensor is mounted deep within a sighting tube which is fixed to the shell such that a line of sight through the sighting tube is at least parallel to the optical axis of the shell. The solar sensor generates a sensor signal which is used as a control input to an actuator control system. End limit switches generate a limit stop signals when the shell reaches maximum angular positions. The actuator control system generates fluid flows to the actuator based the solar sensor signal and the limit stop signals. The method of tracking the sun includes providing a solar cell array, activating the solar collection system when solar radiation illuminating the array exceeds a predetermined threshold, providing a solar sensor shielded from the solar radiation except for direct, aligned radiation, pivotally rotating the shell westward based upon the solar sensor signal, stopping the shell at a maximum angular positions, and rotating the shell westward if the shell does not reach the maximum westward angular orientation during a predetermined daylight time period. The solar energy collection system may be further configured to include a bisected shell, which are hinged together. The shell halves can be collapsed onto each other thereby protecting the light reflective surface and the radiation absorbing segment of the tube carrying heat transfer fluid.

6 Claims, 11 Drawing Sheets

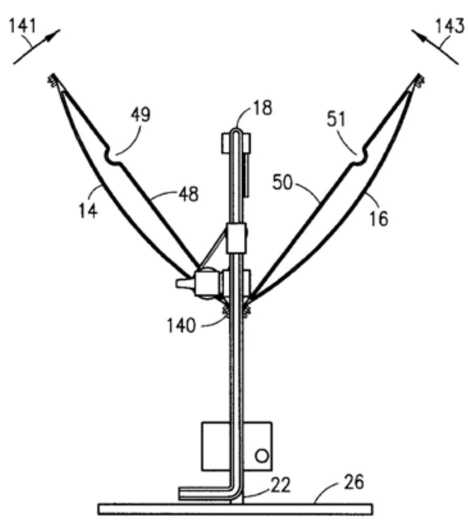

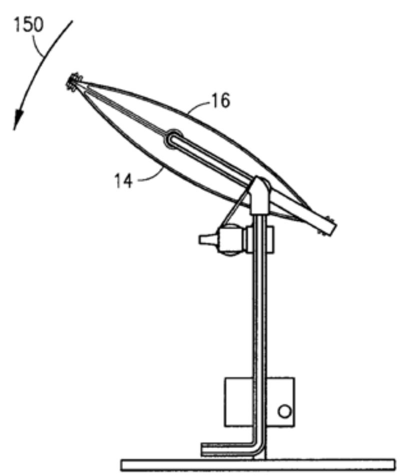

Solar Powered Portable Water Purifier

(12) **United States Patent**
Saraceno

(10) **Patent No.: US 6,863,827 B2**
(45) **Date of Patent: Mar. 8, 2005**

(54) **SOLAR POWERED PORTABLE WATER PURIFIER**

(76) Inventor: **Daniel Saraceno**, 1105 SW. 13^{th} Dr., Boca Raton, FL (US) 33486

(*) Notice: Subject to any disclaimer, the term of this patent is extended or adjusted under 35 U.S.C. 154(b) by 0 days.

(21) Appl. No.: **10/065,999**

(22) Filed: **Dec. 9, 2002**

(65) **Prior Publication Data**

US 2004/0108280 A1 Jun. 10, 2004

(51) **Int. Cl.**^{7} **C02F 1/32**; C02F 9/12

(52) **U.S. Cl.** **210/748**; 210/85; 210/241

(58) **Field of Search** .... 210/748, 85, 205, 210/202, 203, 237, 241, 244, 259, 295; 422/24, 186.3; 250/432 R

(56) **References Cited**

U.S. PATENT DOCUMENTS

5,004,535	A	*	4/1991	Bosko et al.	210/90
5,106,495	A	*	4/1992	Hughes	210/139
5,399,260	A		3/1995	Eldredge et al.	
5,445,729	A	*	8/1995	Monroe et al.	210/86
5,484,538	A	*	1/1996	Woodward	210/767
5,547,584	A		8/1996	Capehart	
6,180,003	B1	*	1/2001	Reber et al.	210/198.1
6,182,453	B1	*	2/2001	Forsberg	62/125
6,193,894	B1	*	2/2001	Hollander	210/748
6,428,694	B1	*	8/2002	Brown	210/170
6,436,283	B1	*	8/2002	Duke	210/172
6,491,811	B2	*	12/2002	Conrad et al.	210/85

FOREIGN PATENT DOCUMENTS

DE 29608545 U1 * 8/1996

* cited by examiner

Primary Examiner—Frank M. Lawrence
(74) *Attorney, Agent, or Firm*—Malin, Haley & DiMaggio, P.A.

(57) **ABSTRACT**

The water purification system and associated method of the present invention consists of a generally self-contained, highly maneuverable, portable water purification system. Maneuverability is enhanced by mounting a cabinet on wheels or on a cart that may be easily guided to a water supply. Power is supplied to the system in a solar cell. The power is used to operate the pump of the system and to power the purifying radiation source. The system can also be used as a portable power source in addition to its capacity as a water purifier.

21 Claims, 3 Drawing Sheets

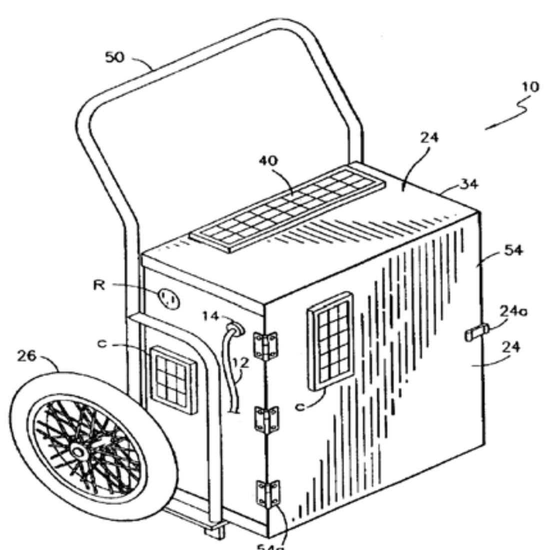

FIG. 2

Sub-Atmospheric Stirring Distillation Device

(19) **United States**
(12) **Patent Application Publication** (10) **Pub. No.: US 2003/0132095 A1**
Kenet et al. (43) **Pub. Date: Jul. 17, 2003**

(54) **DEVICE AND METHOD FOR DISTILLING WATER**

(76) Inventors: **Brian Kenet**, New York, NY (US); **Pedro Joaquin Sanchez Belmar**, Murcia (ES)

Correspondence Address:
DAVIDSON, DAVIDSON & KAPPEL, LLC
485 SEVENTH AVENUE, 14TH FLOOR
NEW YORK, NY 10018 (US)

(21) Appl. No.: **10/047,164**

(22) Filed: **Jan. 15, 2002**

Publication Classification

(51) **Int. Cl.**[7] **B01D 3/10**

(52) **U.S. Cl.** **202/182**; 203/11; 203/24; 203/26; 203/1; 203/DIG. 8444048; 203/DIG. 8444080; 203/DIG. 8444048; 203/23; 202/205; 159/24.1; 159/44; 159/DIG. 8444080; 23/306; 210/512.1; 210/513

(57) **ABSTRACT**

A method for distilling water includes the steps of entering brine to be distilled into a sub-atmospheric boiler having a brine section with a brine output and a water vapor output; concentrating brine in the brine section to a concentration of at least 250 grams of salt or contaminants per liter; stirring the brine in the brine section; and exiting the brine through the brine output. A distiller with a subatmospheric boiler having a stirring device is also provided.

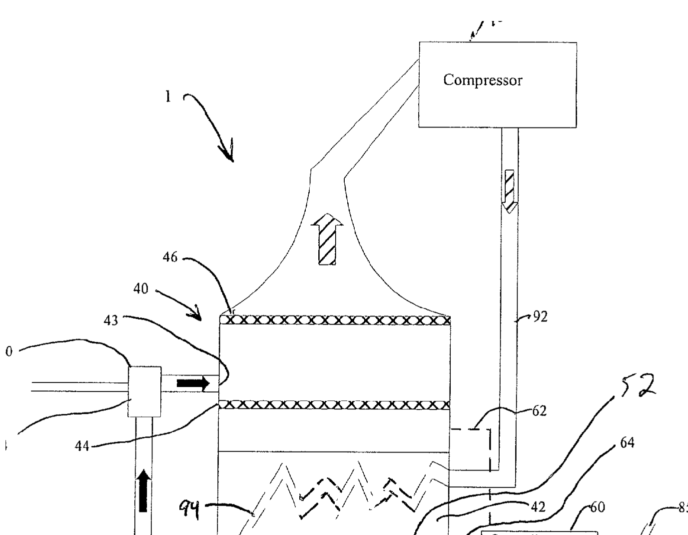

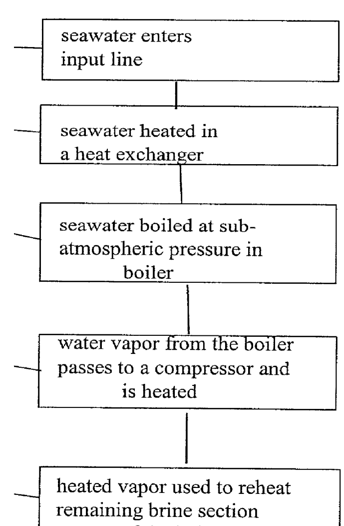

(19) **United States**
(12) **Patent Application Publication** (10) **Pub. No.: US 2004/0055866 A1**
Levine (43) **Pub. Date: Mar. 25, 2004**

(54) **DESALINIZATION STILL**

(76) Inventor: **Michael R. Levine**, Boca Raton, FL (US)

Correspondence Address:
GIFFORD, KRASS, GROH, SPRINKLE
ANDERSON & CITKOWSKI, PC
280 N OLD WOODARD AVE
SUITE 400
BIRMINGHAM, MI 48009 (US)

(21) Appl. No.: **10/665,457**

(22) Filed: **Sep. 19, 2003**

Related U.S. Application Data

(60) Provisional application No. 60/412,230, filed on Sep. 20, 2002. Provisional application No. 60/498,083, filed on Aug. 26, 2003.

Publication Classification

(51) **Int. Cl.**^{7} **B01D 3/10**
(52) **U.S. Cl.** **202/205**; 202/182; 202/236

(57) **ABSTRACT**

A sub-atmospheric pressure desalinating still employs a closed top, opened bottom tank filled with seawater, having a height greater than the height of a column of seawater that can be supported by the pressure at the bottom tank so that a vacuum is formed at the top. A compressor draws vapor from the evacuated area, compresses it and passes it through a heat exchanger within the tank volume to condense the vapor in the tank to generate purified water. Replenishing water is drawn in through the bottom of the tank, passes through a heat exchanger, and is pumped through a heat exchanger coil surrounding the compressor, with the outlet feeding a spray head within the vacuum volume. The compressor and the pump for the intake flow are powered by a wind turbine or wave power.

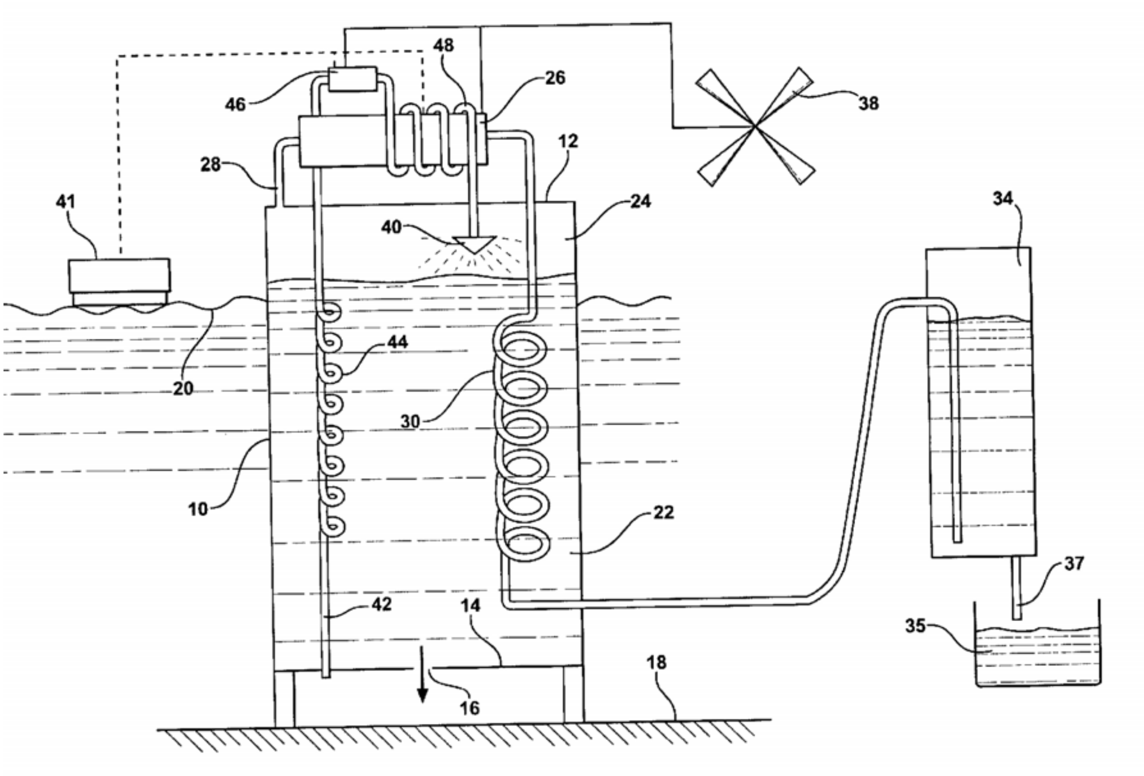

Fuel Cell Powered Desalination Device

(19) **United States**
(12) **Patent Application Publication** (10) **Pub. No.: US 2003/0132097 A1**
Kenet et al. (43) **Pub. Date: Jul. 17, 2003**

(54) **FUEL-CELL POWERED DESALINATION DEVICE**

(76) Inventors: **Brian Kenet**, New York, NY (US); **Pedro Joaquin Sanchez Belmar**, Murcia (ES)

Correspondence Address:
DAVIDSON, DAVIDSON & KAPPEL, LLC
485 SEVENTH AVENUE, 14TH FLOOR
NEW YORK, NY 10018 (US)

(21) Appl. No.: **10/045,560**

(22) Filed: **Jan. 15, 2002**

Publication Classification

(51) **Int. Cl.**^{7} **B01D 3/10**

(52) **U.S. Cl.** **203/11**; 203/24; 203/26; 203/1; 203/23; 203/DIG. 8444048; 203/DIG. 8444080; 202/182; 202/172; 202/205; 159/24.1; 159/44; 159/DIG. 8444048

(57) **ABSTRACT**

A desalination device includes a saltwater input line and a desalinator having a water input connected to the input line, a fresh water output and a brine output. A fuel cell generates electricity and is connected to an energy source for the desalinator. A heat exchanger transfers waste heat from the fuel cell to desalinator.